

The World of Micro/Nano Biomechanics

Tang Bin

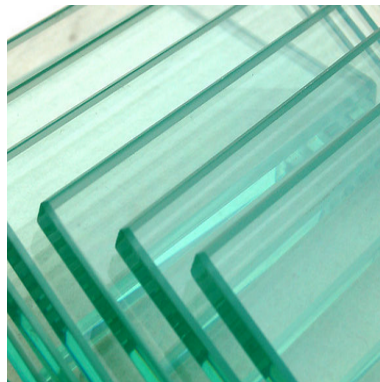
Department of Biomedical Engineering
Southern University of Science and Technology

tang.b@sustc.edu.cn

Why study Mechanical Properties



wood



glass



Titanium



Plastic bag(PP)



Bamboo



ceramic



aluminum



**Plastic chair
(PE)**

Mechanical properties, one group of characteristics of materials, the resistance of materials to plastic/elastic deformation internally/externally.

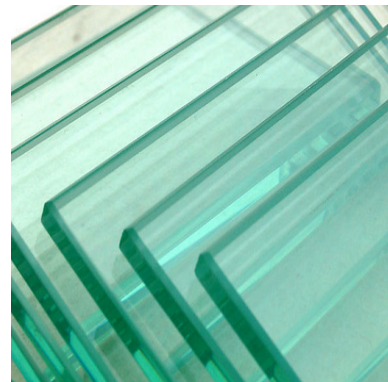
Mechanical support is one of basic function for most of materials, and to understand the mechanical properties of them will help in the engineering design of certain devices.

Mechanical behavior of Materials

Hard- soft -> Hardness

brittle-ductile -> ductility

strong-weak->strength, stiffness....



The mechanical properties of materials can be determined by performing carefully designed laboratory experiments that replicate as nearly as possible the service conditions.

Factors to be considered:

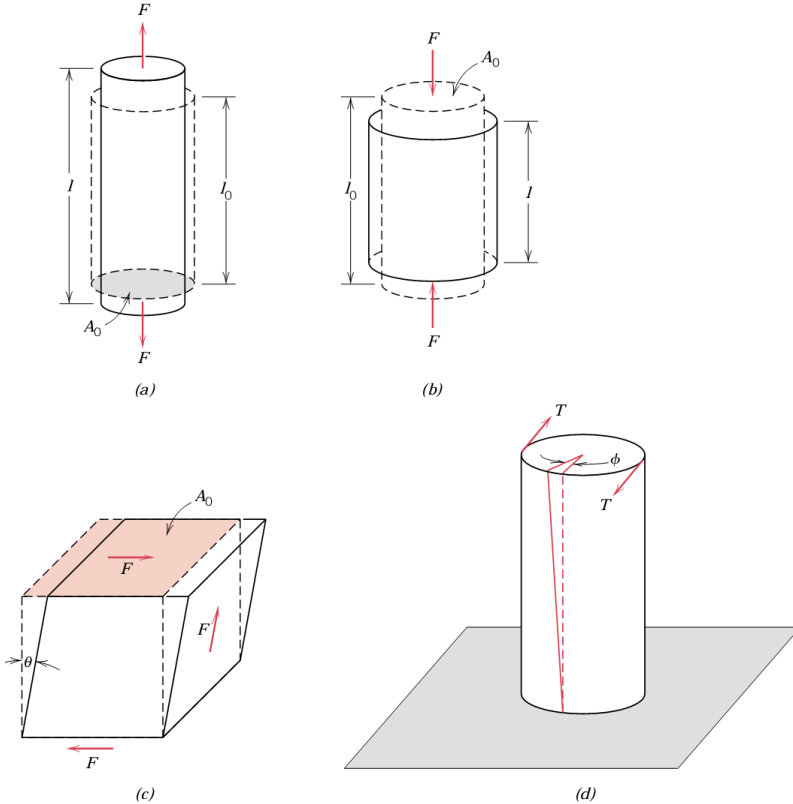
- The nature of the applied load (e.g. tensile, compressive, or shear) and its duration
- Environmental conditions, e.g. service temperature, humidity, etc.

Standards: e.g. ASTM (USA), GB, ISO(China),etc.

Fundamental concept: Stress and Strain

Stress σ : Force per unit area.

Strain ϵ : Relative deformation divided by the reference configuration.



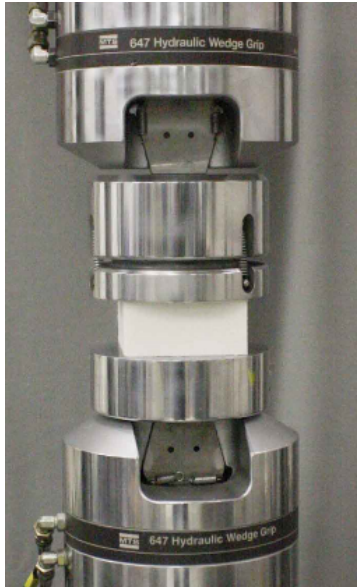
$$\epsilon = \frac{l - l_0}{l_0} = \frac{\Delta l}{l_0}$$

$$\sigma = \frac{F}{A_0}$$

Commonly seen deformation: **tension, compression, shear, and torsion**

Compression test

Compression stress–strain tests may be conducted if in-service forces are of this type. A compression test is conducted in a manner similar to the tensile test, except that the force is compressive and the specimen contracts along the direction of the stress.



$$\sigma = \frac{F}{A_0}$$

$$\epsilon = \frac{l_i - l_0}{l_0} = \frac{\Delta l}{l_0}$$

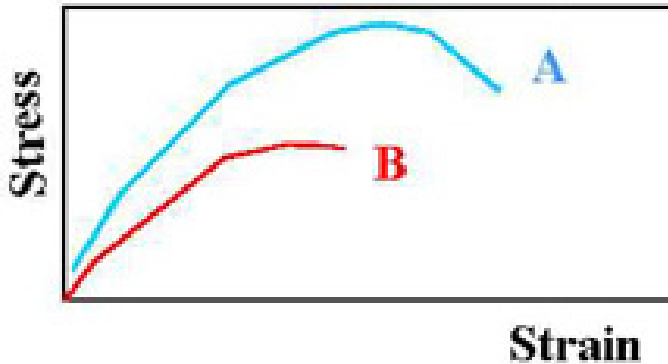
1. same calculation equations as those in tensile test
2. a compressive force is taken to be negative, which yields a negative stress
3. original length l_0 is large than instantaneous length l_i , so the strain is negative too, and so the measured mechanical properties is still positive (stress/strain).

Compressive tests are used when a material's behavior under large and permanent (i.e., plastic) strains is desired, as in manufacturing applications, or when the material is brittle in tension.

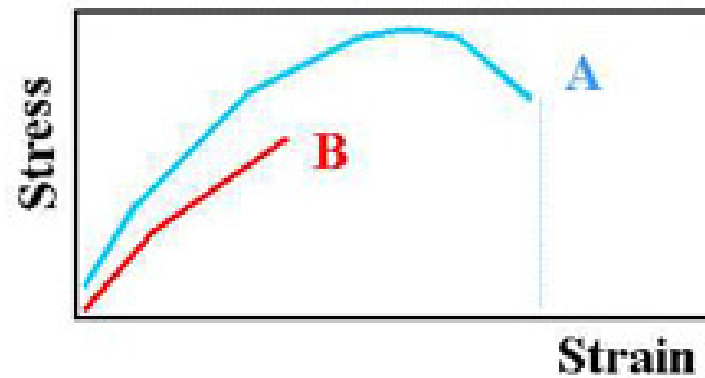
Real practices



Which material is stronger?



Which material is ductile?

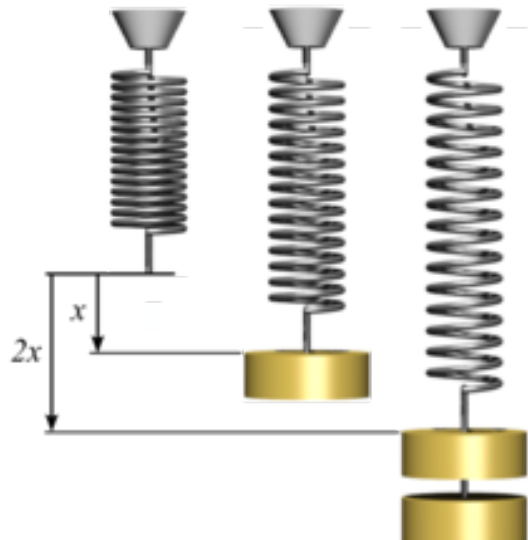


Stress-strain behavior

$$\sigma = E\epsilon$$

Hooke's law

If stress the materials in low levels, the applied stress and strain are proportional to each other, and this is called Hooke's law, Deformation of materials obey Hooke's law is known as elastic deformation(**this type of deformation will recover after the release of applied stress**), the ratio between the stress and strain ratio, i.e. the E value shown above, is call elastic modulus, or Young's modulus.



$$G = \frac{\tau}{\gamma}$$

Same as elastic modulus, the shear modulus is defined as the applied stress devided by the shear strain

Table 7.1 Room-Temperature Elastic and Shear Moduli, and Poisson's Ratio for Various Materials

Material	Modulus of Elasticity		Shear Modulus		Poisson's Ratio
	GPa	10 ⁶ psi	GPa	10 ⁶ psi	
Metal Alloys					
Tungsten	407	59	160	23.2	0.28
Steel	207	30	83	12.0	0.30
Nickel	207	30	76	11.0	0.31
Titanium	107	15.5	45	6.5	0.34
Copper	110	16	46	6.7	0.34
Brass	97	14	37	5.4	0.34
Aluminum	69	10	25	3.6	0.33
Magnesium	45	6.5	17	2.5	0.35
Ceramic Materials					
Aluminum oxide (Al_2O_3)	393	57	—	—	0.22
Silicon carbide (SiC)	345	50	—	—	0.17
Silicon nitride (Si_3N_4)	304	44	—	—	0.30
Spinel (MgAl_2O_4)	260	38	—	—	—
Magnesium oxide (MgO)	225	33	—	—	0.18
Zirconia ^a	205	30	—	—	0.31
Mullite ($3\text{Al}_2\text{O}_3\text{-}2\text{SiO}_2$)	145	21	—	—	0.24
Glass-ceramic (Pyroceram)	120	17	—	—	0.25
Fused silica (SiO_2)	73	11	—	—	0.17
Soda-lime glass	69	10	—	—	0.23
Polymers^b					
Phenol-formaldehyde	2.76–4.83	0.40–0.70	—	—	—
Polyvinyl chloride (PVC)	2.41–4.14	0.35–0.60	—	—	0.38
Polyester (PET)	2.76–4.14	0.40–0.60	—	—	—
Polystyrene (PS)	2.28–3.28	0.33–0.48	—	—	0.33
Polymethyl methacrylate (PMMA)	2.24–3.24	0.33–0.47	—	—	—
Polycarbonate (PC)	2.38	0.35	—	—	0.36
Nylon 6,6	1.58–3.80	0.23–0.55	—	—	0.39
Polypropylene (PP)	1.14–1.55	0.17–0.23	—	—	—
Polyethylene—high density (HDPE)	1.08	0.16	—	—	—
Polytetrafluoroethylene (PTFE)	0.40–0.55	0.058–0.080	—	—	0.46
Polyethylene—low density (LDPE)	0.17–0.28	0.025–0.041	—	—	—

^a Partially stabilized with 3 mol% Y_2O_3 .

^b Source: *Modern Plastics Encyclopedia '96*. Copyright 1995, The McGraw-Hill Companies. Reprinted with permission.

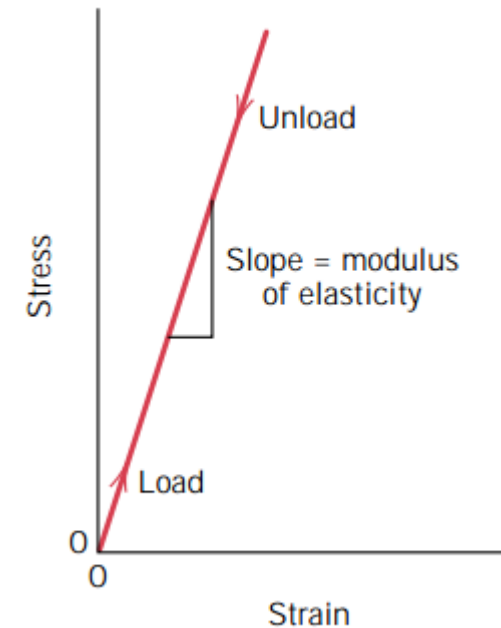
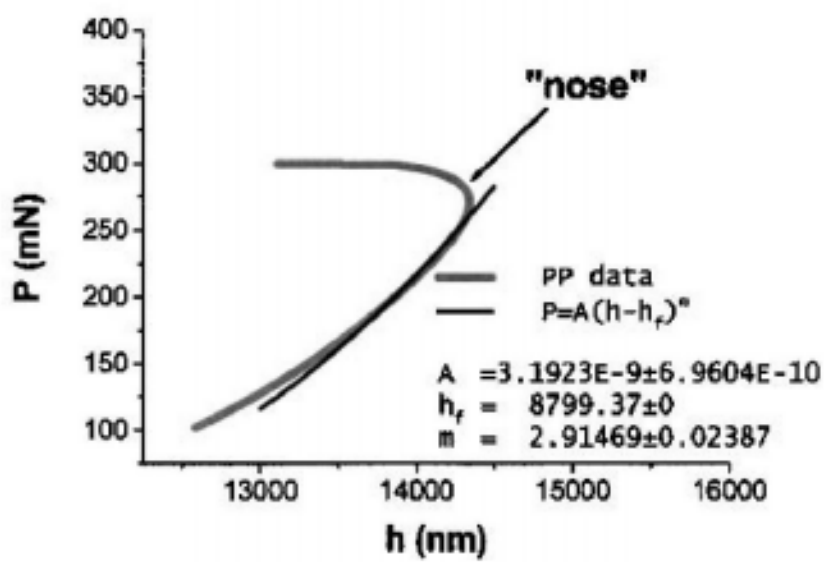
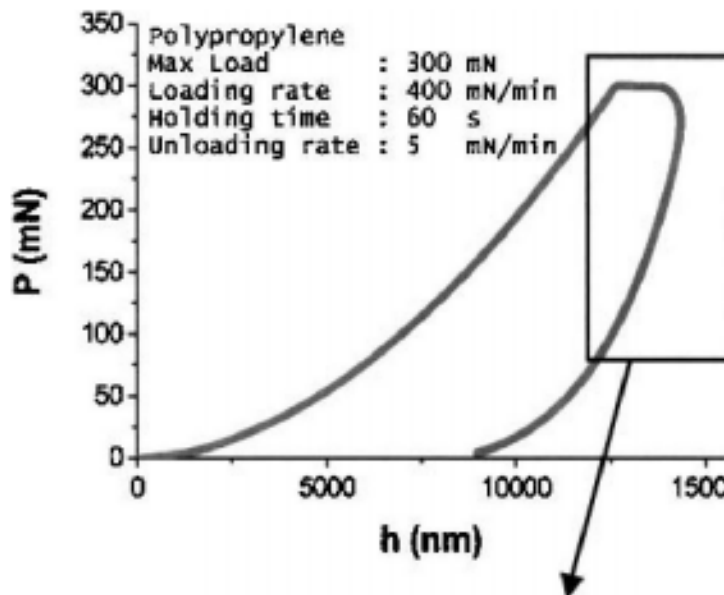


FIGURE 7.5 Schematic stress-strain diagram showing linear elastic deformation for loading and unloading cycles.



Deformation will continue after the stress application, and upon load release some finite time is required for complete recovery. This time-dependent elastic behavior is known as **anelasticity**, and it is due to time-dependent microscopic and atomistic processes that are attendant to the deformation. For metals the anelastic component is normally small and is often neglected (**it will be quite significant under high stress, or the temperature is high**), the anelastic deformation of metal including plastic and creep). However, for some polymeric materials its magnitude is significant; in this case it is termed viscoelastic behavior,

Elastic Properties of Materials - Possion's ratio

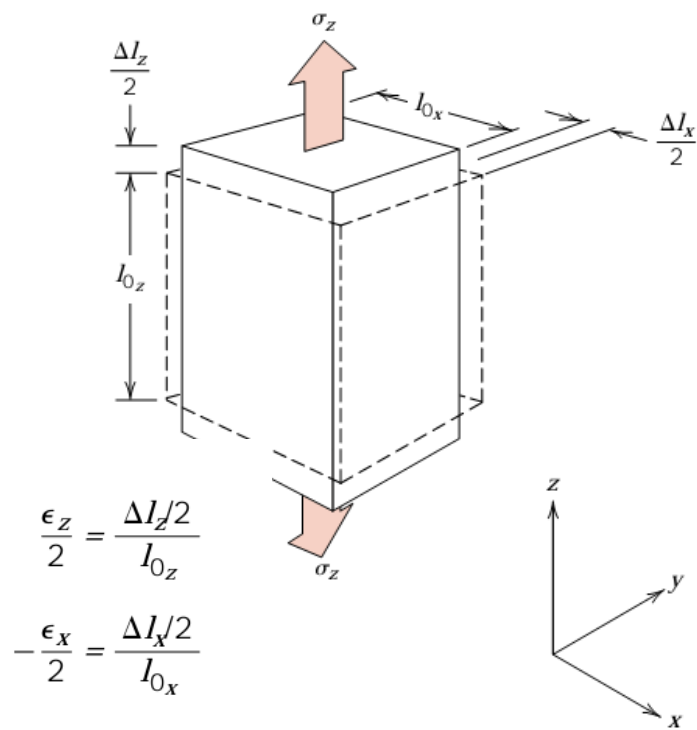


FIGURE 7.9 Axial (z) elongation (positive strain) and lateral (x and y) contractions (negative strains) in response to an imposed tensile stress. Solid lines represent dimensions after stress application; dashed lines, before.

$$E = 2G(1 + \nu)$$

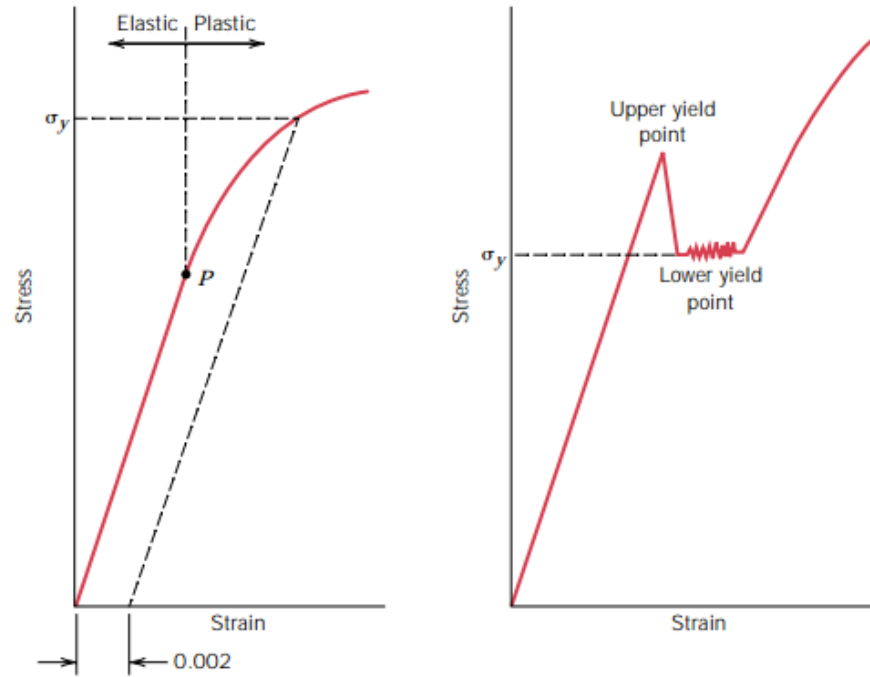
Only for isotropic materials

$$\nu = -\frac{\epsilon_x}{\epsilon_z} = -\frac{\epsilon_y}{\epsilon_z}$$

Poisson's ratio, the ratio of the lateral and axial strains. For many metals and other alloys, values of Poisson's ratio range between 0.25 and 0.35.

Yield strength

FIGURE 7.10
(a) Typical stress-strain behavior for a metal showing elastic and plastic deformations, the proportional limit P , and the yield strength σ_y , as determined using the 0.002 strain offset method.
(b) Representative stress-strain behavior found for some steels demonstrating the yield point phenomenon.



Plastic deformation: As the material is deformed beyond its ^(a)elastic limit, the stress is no longer proportional to strain (the crystal structure change permanently), and permanent, nonrecoverable deformation happen.

Yield strength is the stress at which **the plastic deformation happen (yielding point)**

0.002 strain offset method (*or other strain may be used in particularly case*), is to draw a line parallel to the linear stress-strain curve at give strain, and find out the intersection of this line and the stress-strain curve, which is the yield strength.

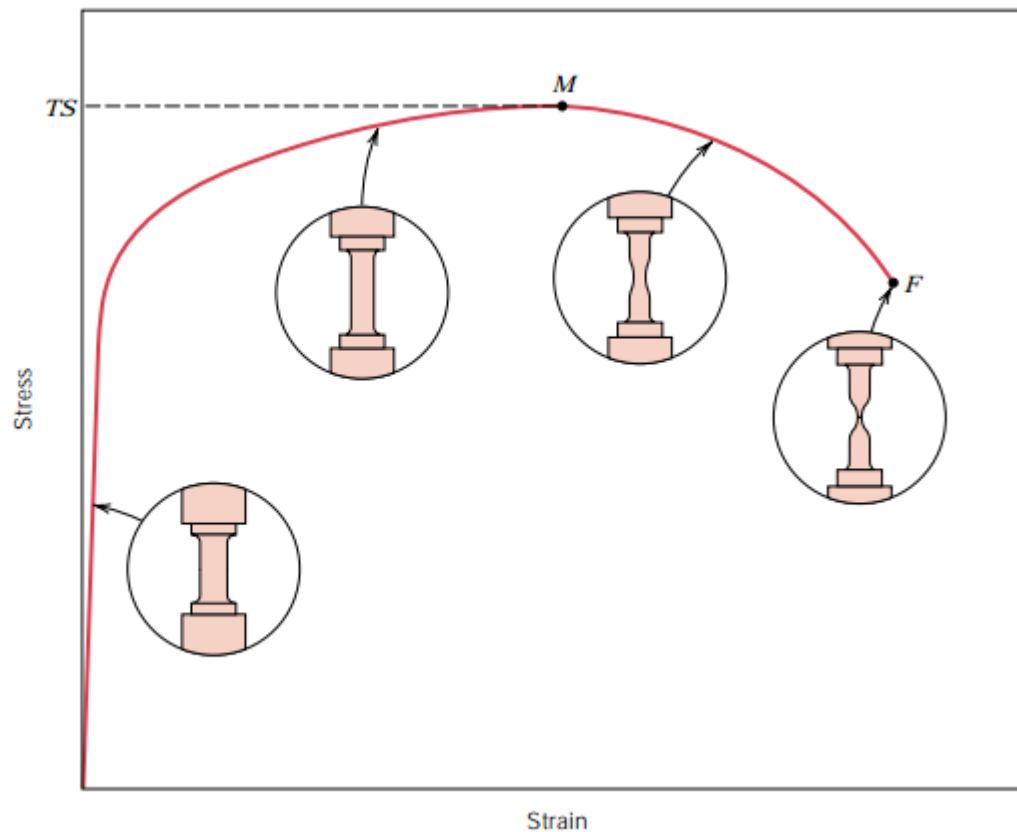
For materials with nonlinear elastic region, The yield strength is defined as the stress required to produce some amount of strain

For special case shown in fig. (b), the yield strength is the average of the upper and lower one.

Tensile strength

FIGURE 7.11
Typical engineering stress-strain behavior to fracture, point *F*. The tensile strength *TS* is indicated at point *M*.

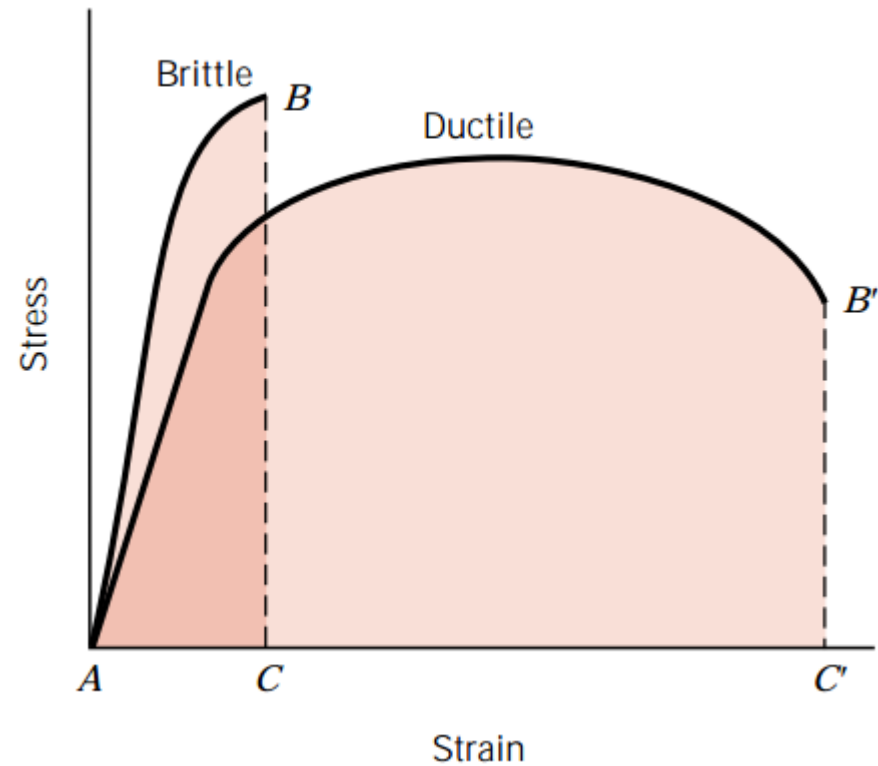
The circular insets represent the geometry of the deformed specimen at various points along the curve.



The **tensile strength** (TS) is the stress at the maximum on the engineering stress-strain curve, a small constriction or neck begins to form at some point, and all subsequent deformation is confined at this neck, this is call necking.

Remember: Use the yield strength but not the tensile strength when doing engineering design.

Toughness



Toughness is a mechanical term, in general, represent the ability of a material to absorb energy up to fracture. notch toughness is assessed by using an impact test. For a material to be tough, it must display both strength and ductility; and often, **ductile materials are tougher than brittle ones.**

ELASTIC RECOVERY DURING PLASTIC DEFORMATION

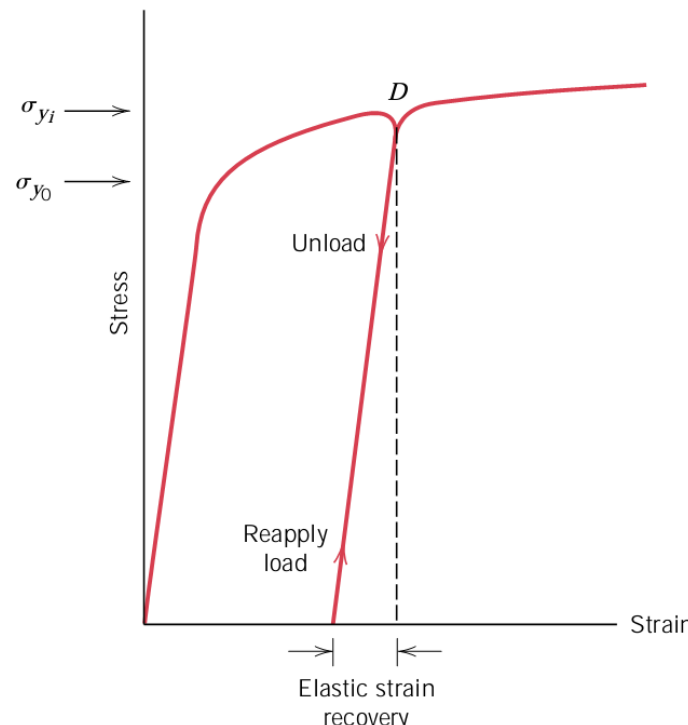
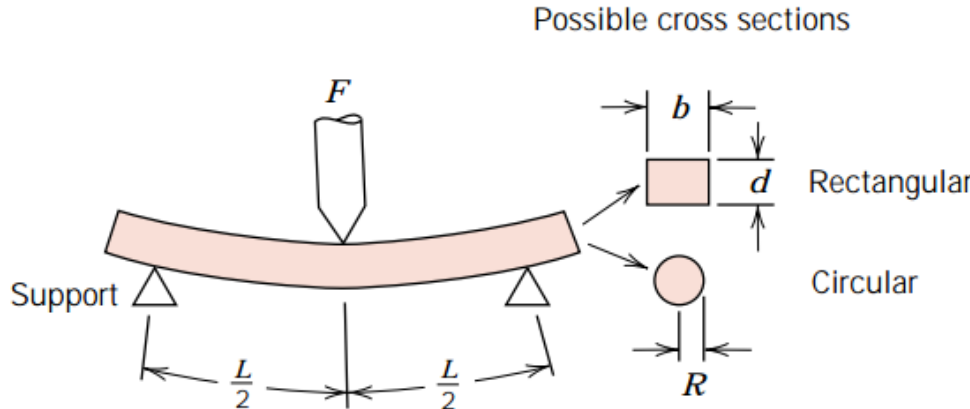


FIGURE 7.17 Schematic tensile stress-strain diagram showing the phenomena of elastic strain recovery and strain hardening. The initial yield strength is designated as σ_{y_0} ; σ_{y_i} is the yield strength after releasing the load at point D, and then upon reloading.

Deformation:
Elastic+plastic+viscoelastic

Upon release of the load during the course of a stress-strain test, some fraction of the total deformation is recovered as elastic strain, as shown above. During the unloading cycle, the curve traces a near straight-line path from the point of unloading (point D), and its slope is virtually identical to the modulus of elasticity, or parallel to the initial elastic portion of the curve. The magnitude of this elastic strain, which is regained during unloading, corresponds to the strain recovery. ***If the load is reapplied, the curve will traverse essentially the same linear portion in the direction opposite to unloading; yielding will again occur at the unloading stress level where the unloading began.*** There will also be an elastic strain recovery associated with fracture.

Flexural strength



$$\sigma = \text{stress} = \frac{Mc}{I}$$

where M = maximum bending moment

c = distance from center of specimen
to outer fibers

I = moment of inertia of cross section

F = applied load

	\underline{M}	\underline{c}	\underline{I}	$\underline{\sigma}$
Rectangular	$\frac{FL}{4}$	$\frac{d}{2}$	$\frac{bd^3}{12}$	$\frac{3FL}{2bd^2}$

Circular	$\frac{FL}{4}$	R	$\frac{\pi R^4}{4}$	$\frac{FL}{\pi R^3}$
----------	----------------	-----	---------------------	----------------------

FIGURE 7.18 A three-point loading scheme for measuring the stress-strain behavior and flexural strength of brittle ceramics, including expressions for computing stress for rectangular and circular cross sections.

$$\sigma_{fs} = \frac{3F_fL}{2bd^2} \quad \text{rectangular}$$

$$\sigma_{fs} = \frac{F_fL}{\pi R^3} \quad \text{circular}$$

Bending tests usually is applied to ceramics:

hard, so it is difficult to prepare and test specimens having the required geometry.
brittle, it is difficult to grip without fracturing them

Elongation is very small, ceramics fail after only about 0.1% strain

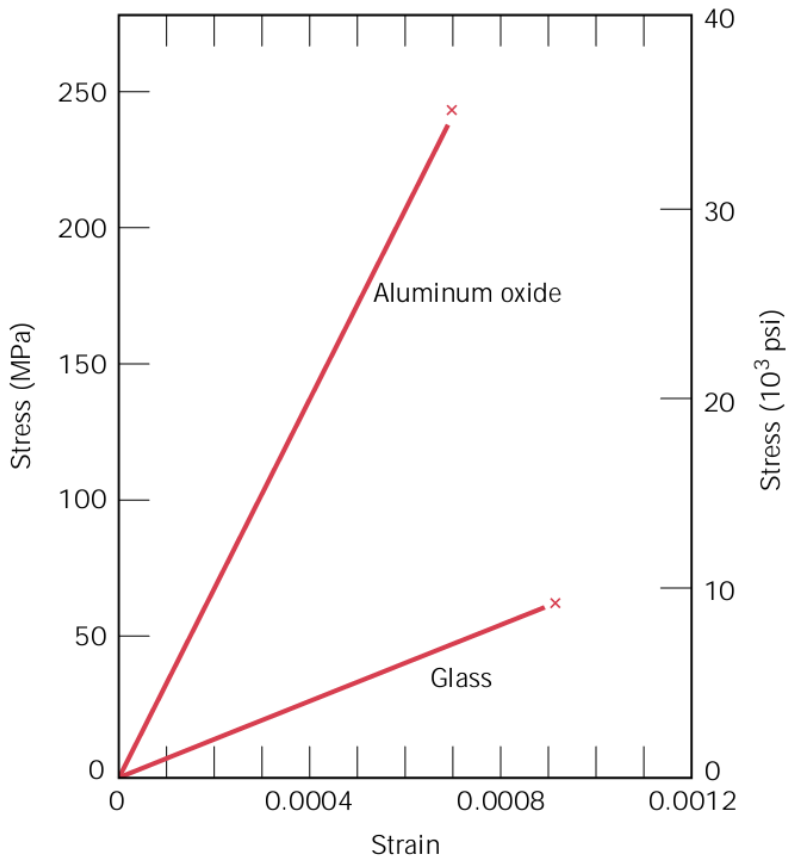
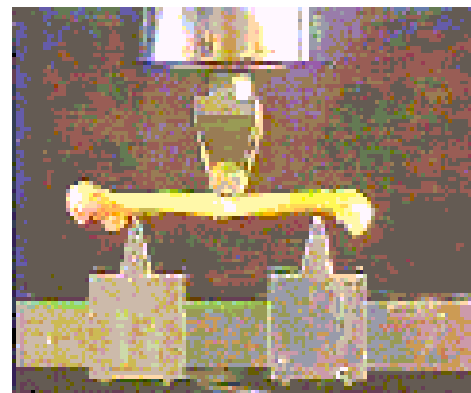


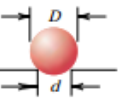
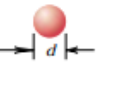
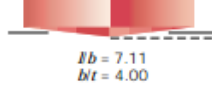
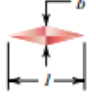
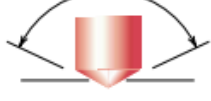
FIGURE 7.19 Typical stress–strain behavior to fracture for aluminum oxide and glass.



The magnitude of its flexural strength is greater than the tensile fracture strength, and it is **depend on specimen size**.

Hardness

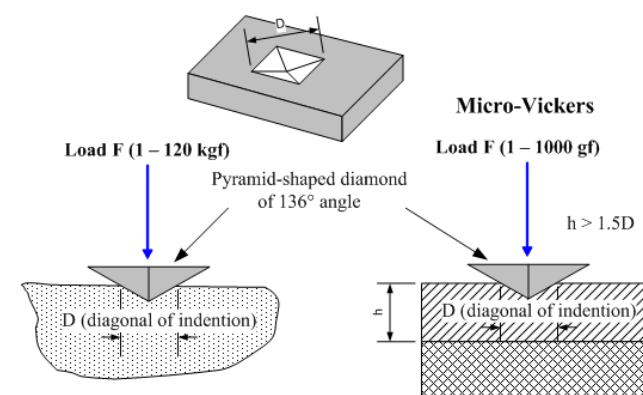
Table 7.4 Hardness Testing Techniques

Test	Indenter	Shape of Indentation	Side View	Top View	Load	Formula for Hardness Number ^a
Brinell	10-mm sphere of steel or tungsten carbide				P	$HB = \frac{2P}{\pi D[D - \sqrt{D^2 - d^2}]}$
Vickers microhardness	Diamond pyramid				P	$HV = 1.854 P/d_1^2$
Knoop microhardness	Diamond pyramid				P	$HK = 14.2 P/l^2$
Rockwell and Superficial Rockwell	Diamond cone $\frac{1}{16}, \frac{1}{8}, \frac{1}{4}, \frac{1}{2}$ in. diameter steel spheres					60 kg 100 kg 150 kg 15 kg 30 kg 45 kg
						Rockwell Superficial Rockwell

^a For the hardness formulas given, P (the applied load) is in kg, while D , d , d_1 , and l are all in mm.

Source: Adapted from H. W. Hayden, W. G. Moffatt, and J. Wulff, *The Structure and Properties of Materials*, Vol. III, *Mechanical Behavior*. Copyright © 1965 by John Wiley & Sons, New York. Reprinted by permission of John Wiley & Sons, Inc.

Vickers Hardness Test

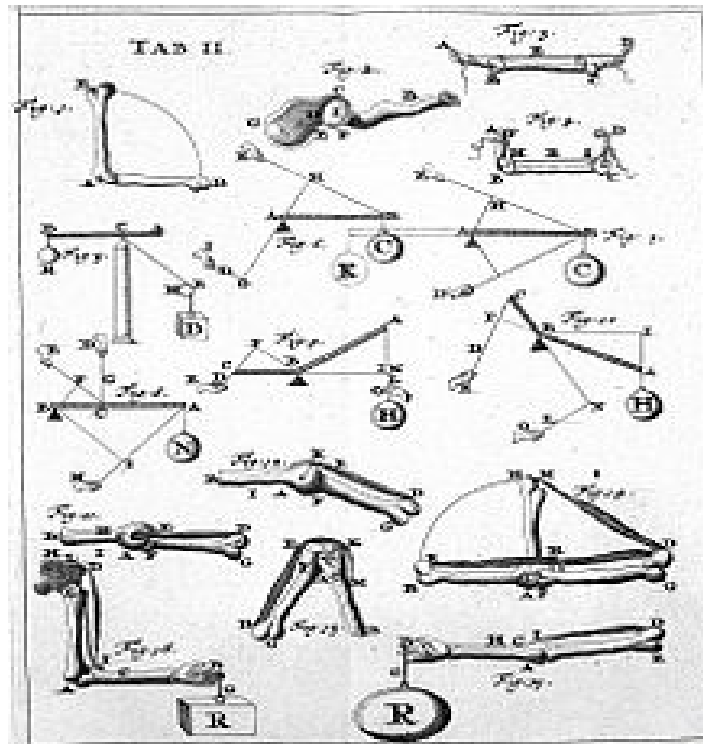


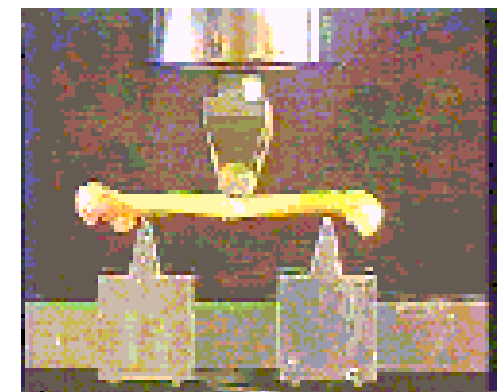
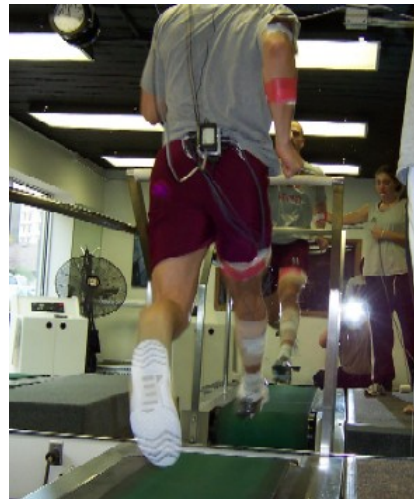
Hardness is a measure of a material's resistance to localized plastic deformation.

$$H=P/A$$

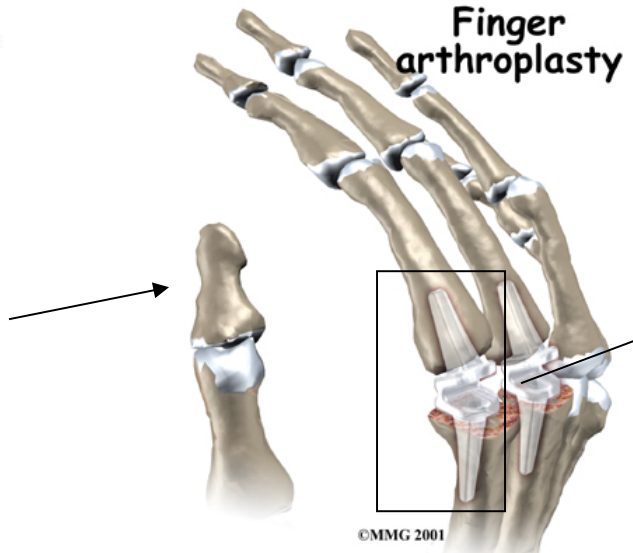
Biomechanics

Biomechanics is the study of the structure and function of biological systems such as humans, animals, plants, organs, and cells by means of the methods of mechanics.



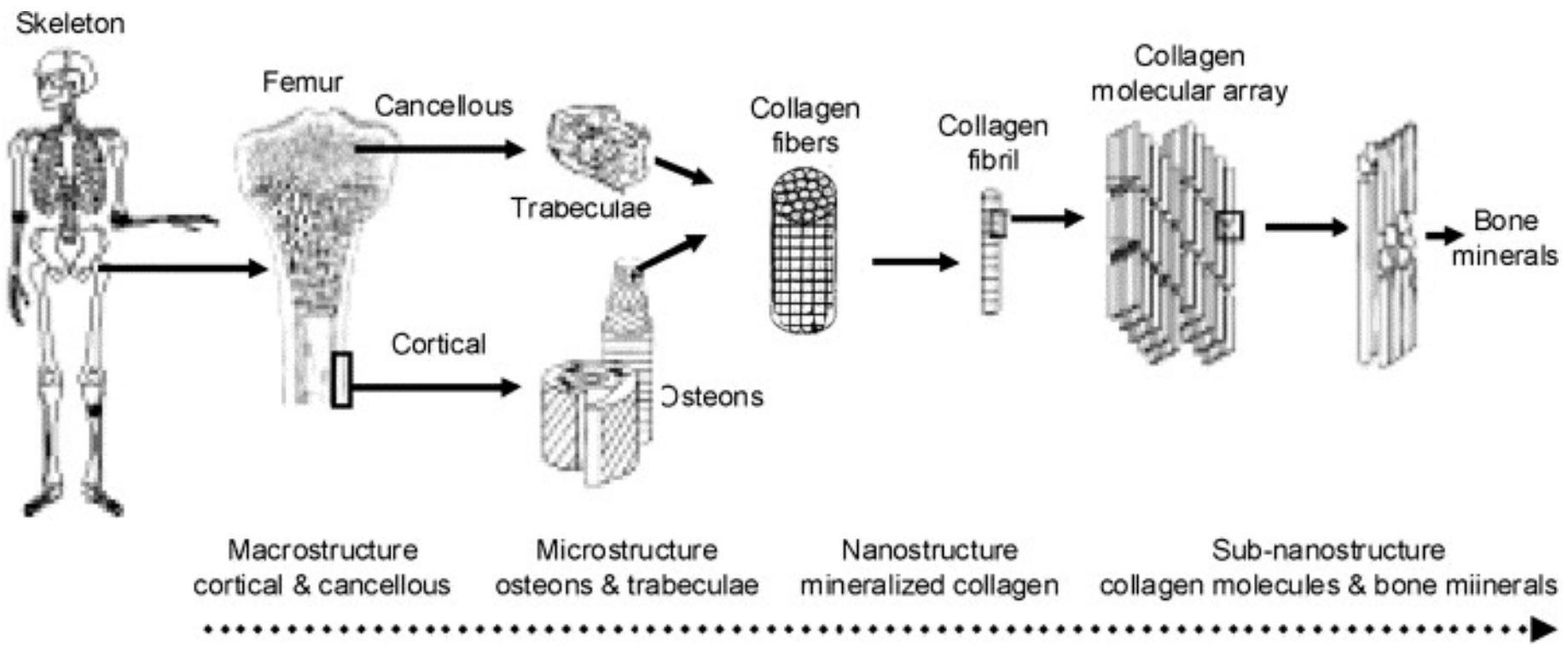


Traditional methods, such as bending, tensile, etc., can only measure the bulk mechanical properties.

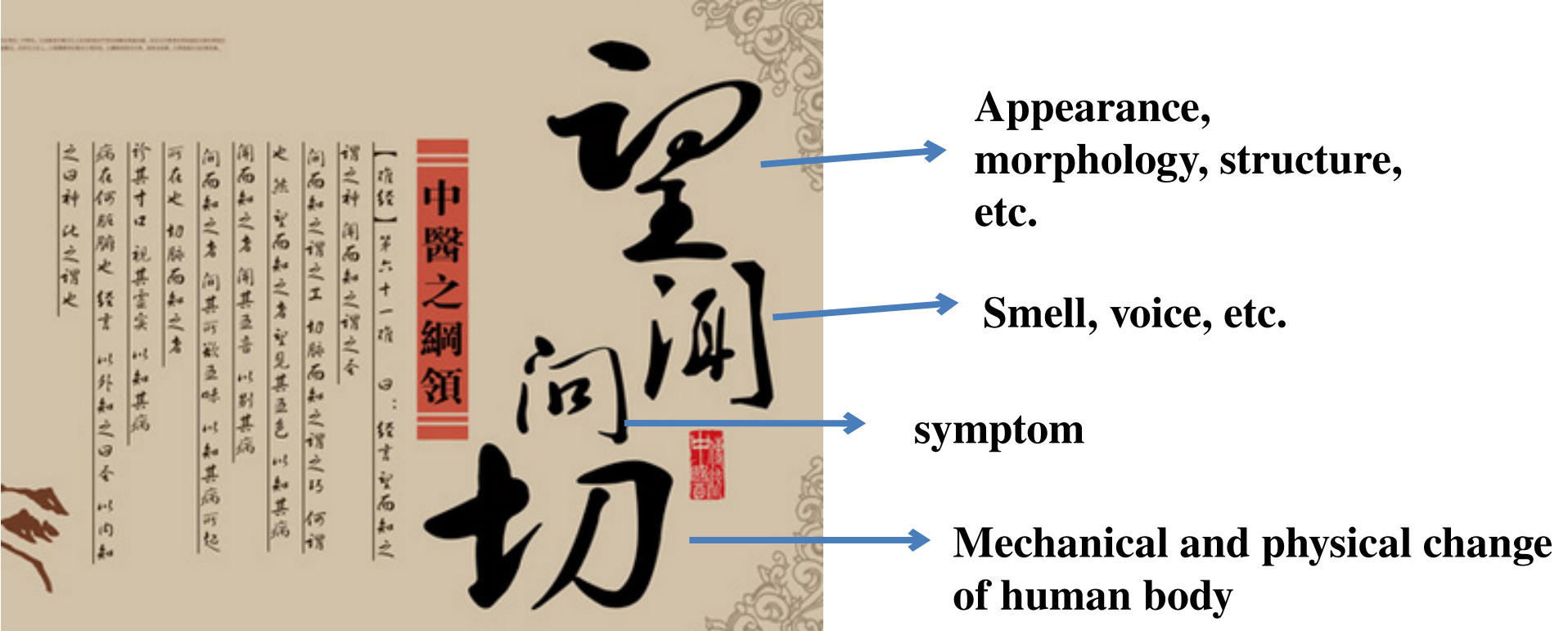


Implant design requires LOCAL properties.

The hierarchical structure of bone



The micro/nano mechanical properties of the “bricks” of human are desired to be known, in bone, the basic structural unit is Hydroxyapatite and collagen fibrils.

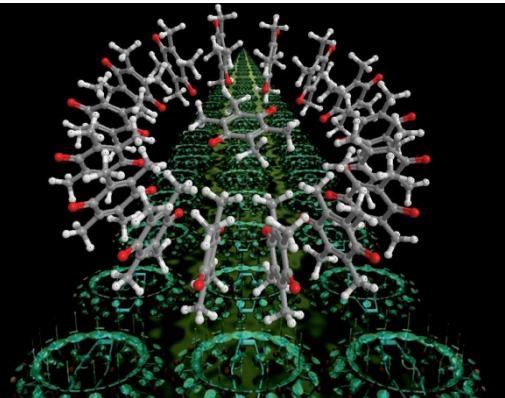


The biomechanical properties of biological tissues are directly determined by their structure and composition. In human body, various physiological change during the progression of diseases may lead to the change of biomechanical/physical properties of relevant cells or tissues: the chondrocytes from the patient suffering osteoarthritis are significant soft than those from the health person, cancer cells are much easier to be deformed than the health cells, the red blood cells harvested from malaria patients are much stiffer than the normal red blood cells.

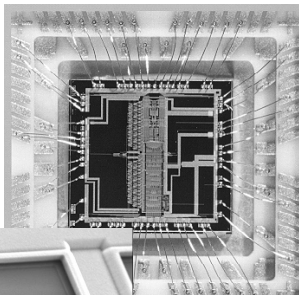
Physical and mechanical change of the “bricks”
 -----The genetic/chemical change of basic unit of tissues --□ The change of physiological function of tissues -> diseases

Technology at Different Length Scales

NEMS



IC



MEMS



μ Robots



Macro Structures



← 0.1nm

1nm

1 μ m

1mm

1m

1km

?? Tools ??

Wavelength of light



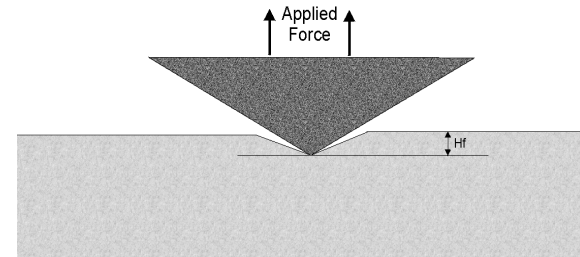
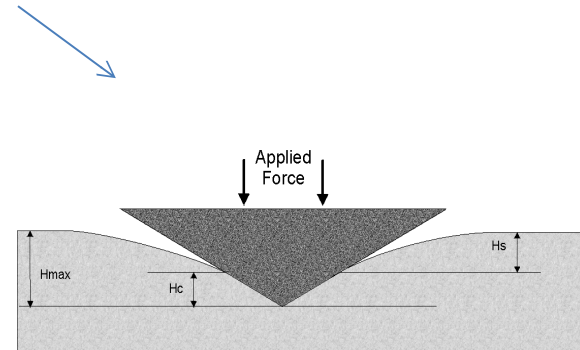
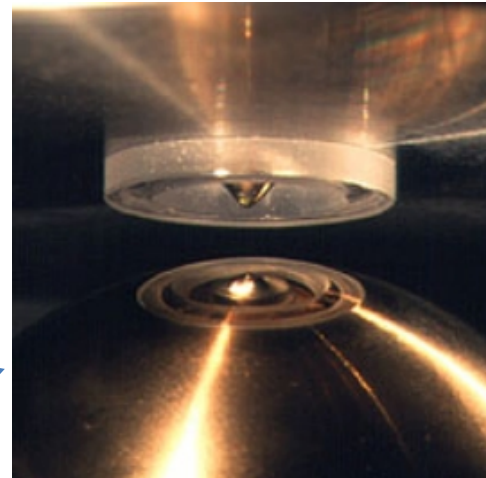
Optical Microscope



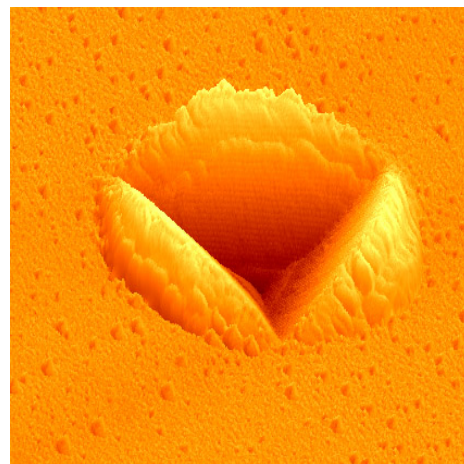
Engineer's Traditional Tools

(Pictures from internet)

Depth-sensing indentation (nanoindentation)



Force, displacement, and time data during indentation are collected and analyzed by certain methods to work out the mechanical properties of elastic modulus, hardness and viscosity



Atomic force microscope

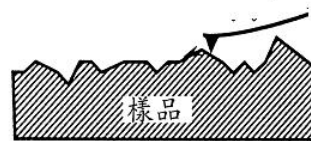


圖 3-9 接觸式掃描方式

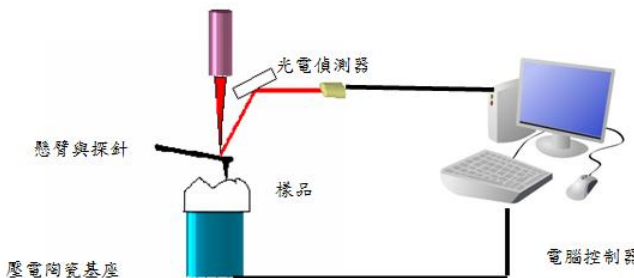
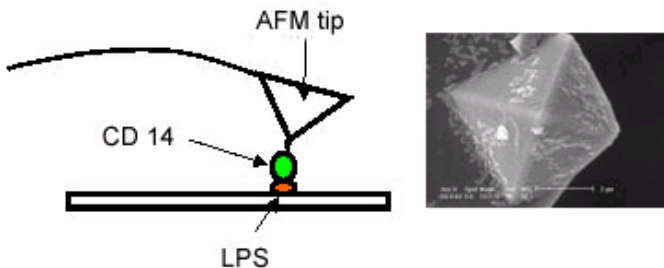
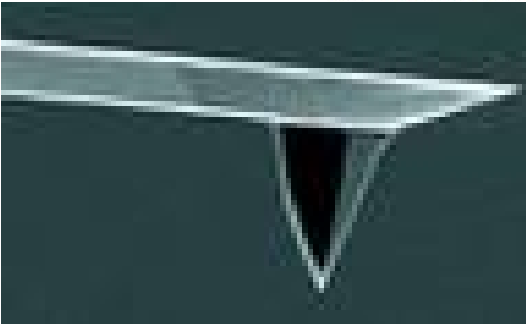
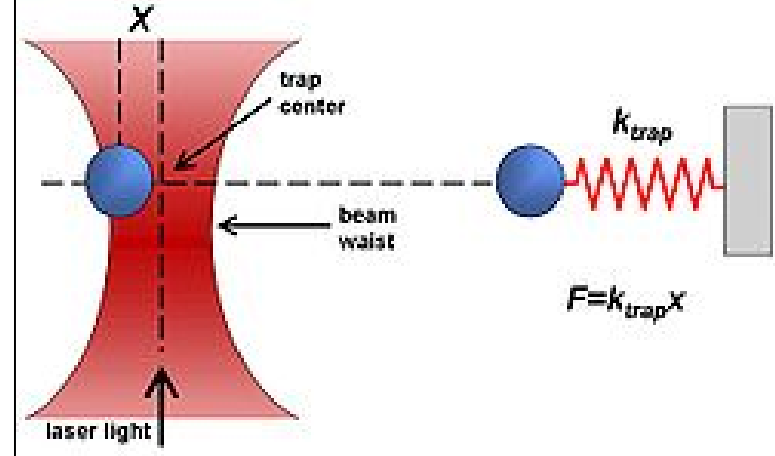
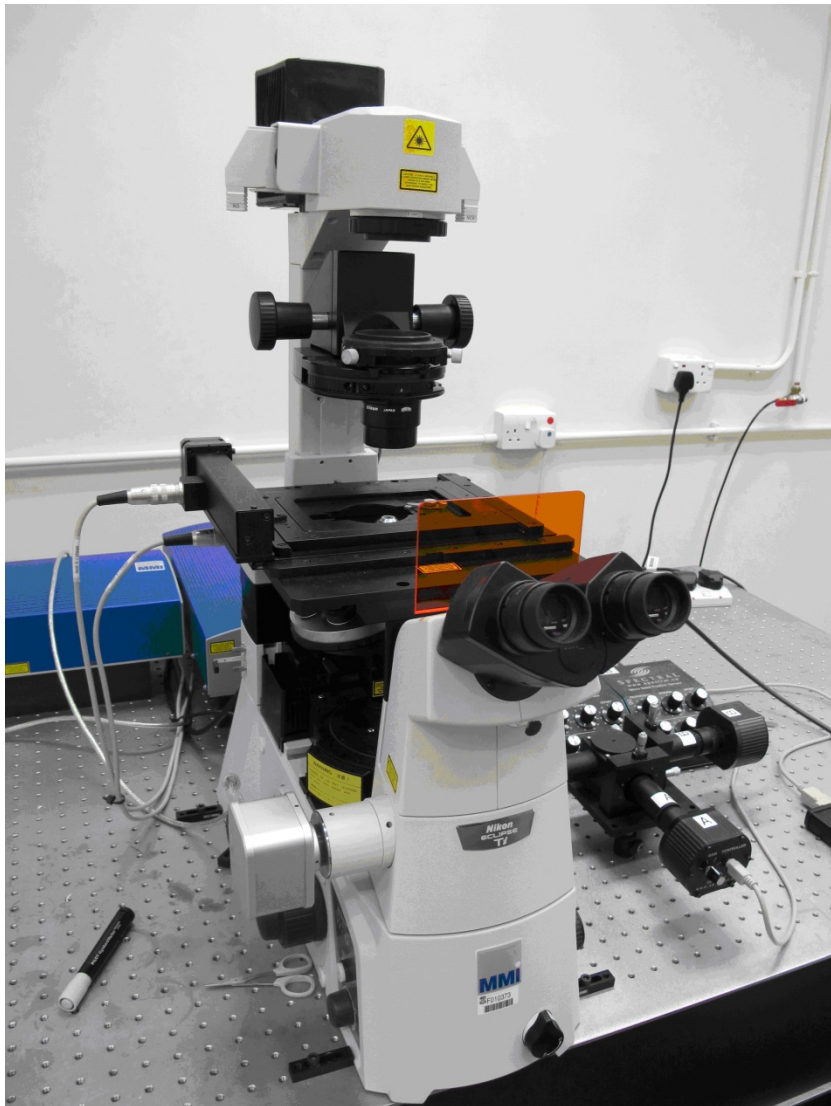


圖 3 AFM 的基本架構示意圖。

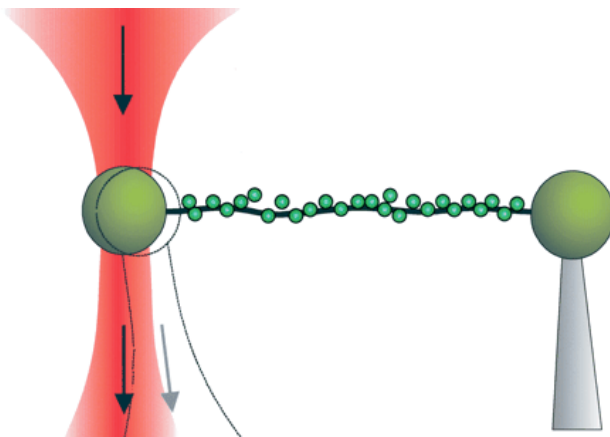


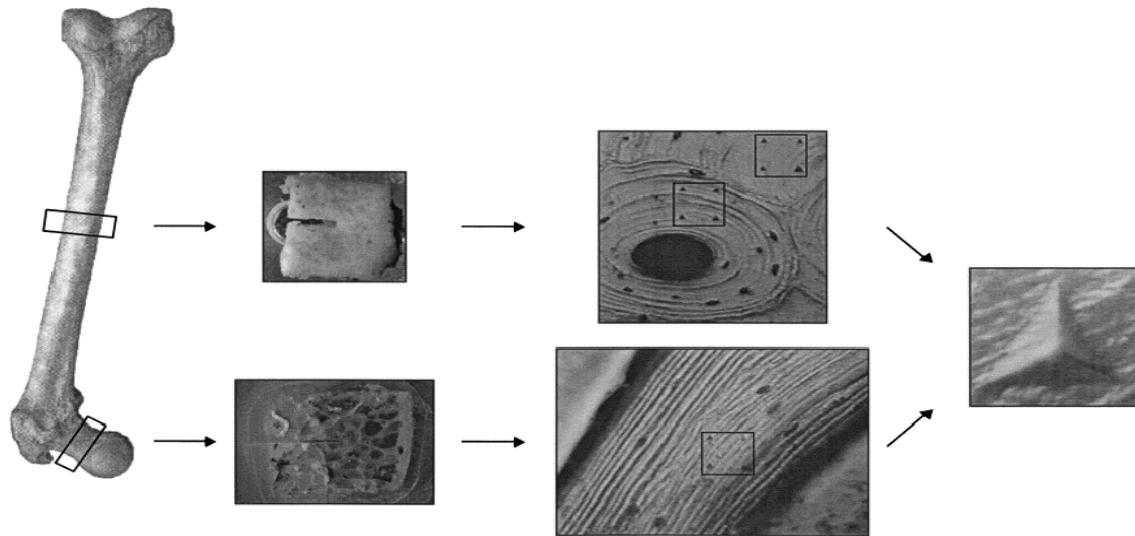
Investigating molecular interaction between white blood cells & bacteria that leads to septic shock using AFM

Optical tweezers



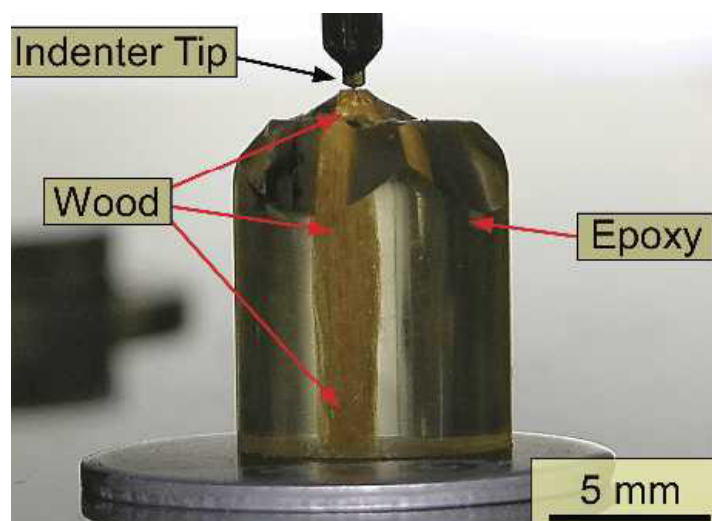
The basic physical principle underlying optical tweezers (OT) is the radiation pressure exerted by light when colliding with matter. The effect was postulated and first demonstrated by Arthur Ashkin in the late 1960s. It has become known as optical trapping, in which dielectric particles can be stably trapped in three dimensions in a tightly focused laser beam



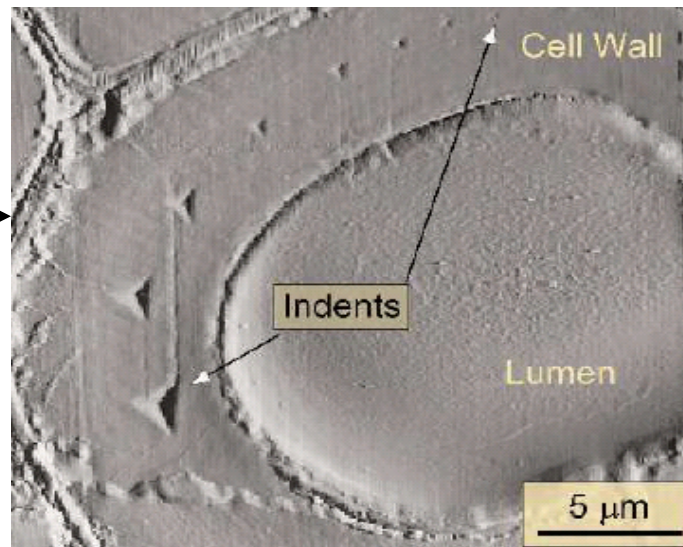


Zysset et al., 1999, *Journal of Biomechanics*.

A Comparison between human femur cortical and trabecular bone.



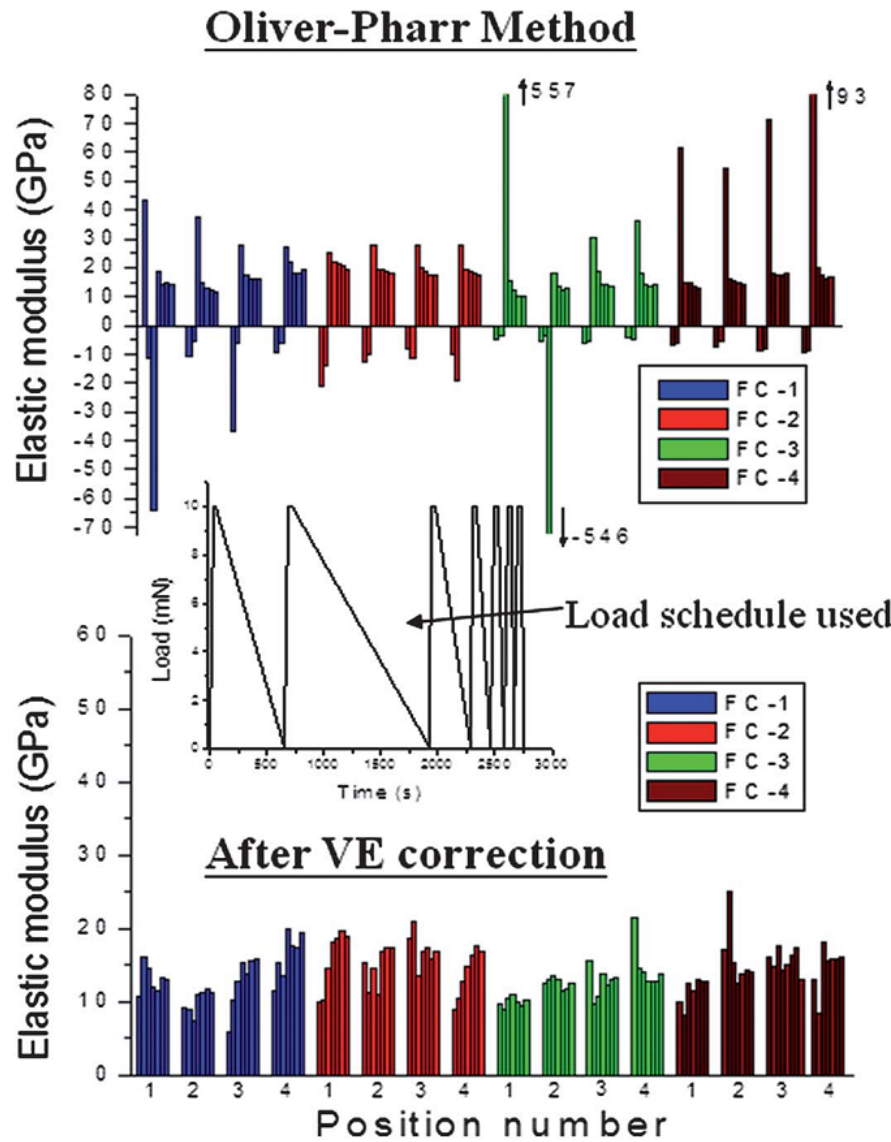
Embedded wood sample.



Indentations on wood.

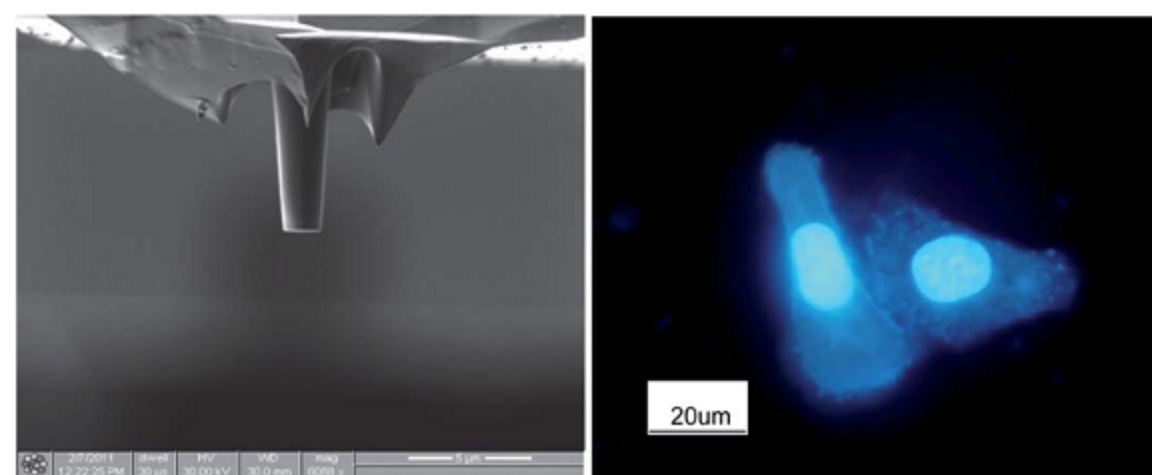
Moon et al., 2006
Forest Products Journal.

Specific method for biological tissues: Rate jump method for different mechanical testing platforms

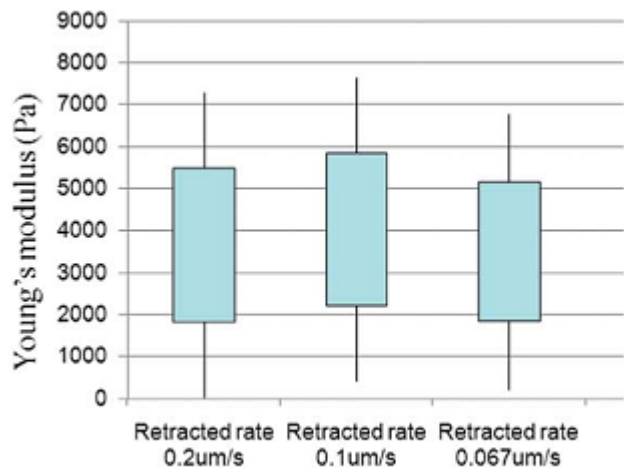
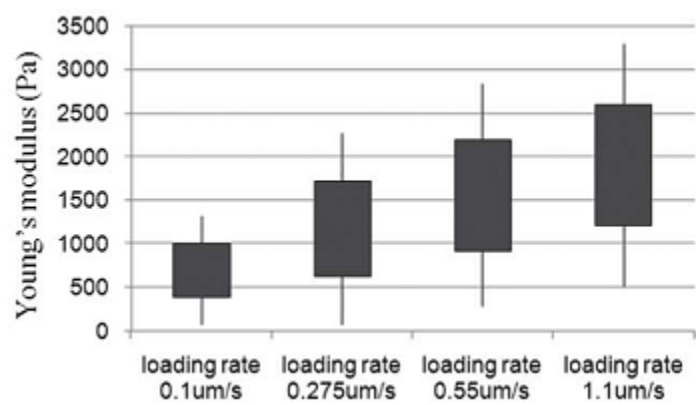


$$\frac{1}{S_e} = \frac{1}{2E_r a} = \frac{\dot{\Delta h}}{\dot{\Delta P}} = \frac{1}{S} - \frac{\dot{h}_h}{\dot{P}_u},$$

*rate-jump method for
Depth-sensing
indentation*

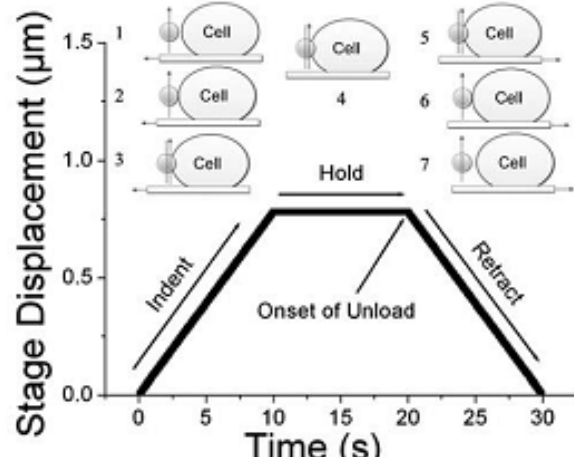
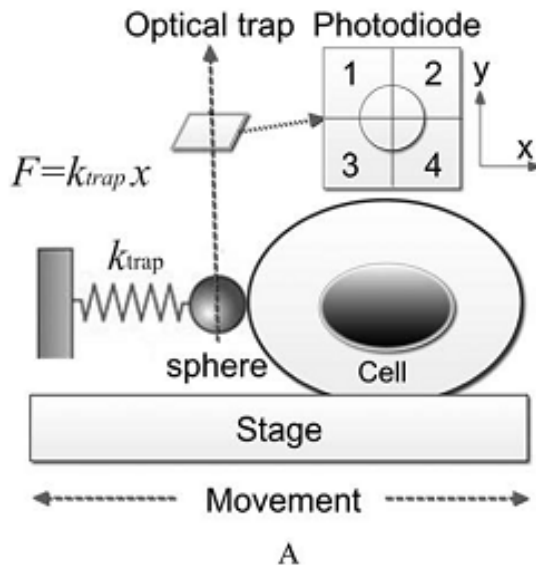


$$\frac{\dot{\Delta\delta}}{\dot{\Delta D}} = A \left(1 + \frac{\alpha}{E_r} \right)$$

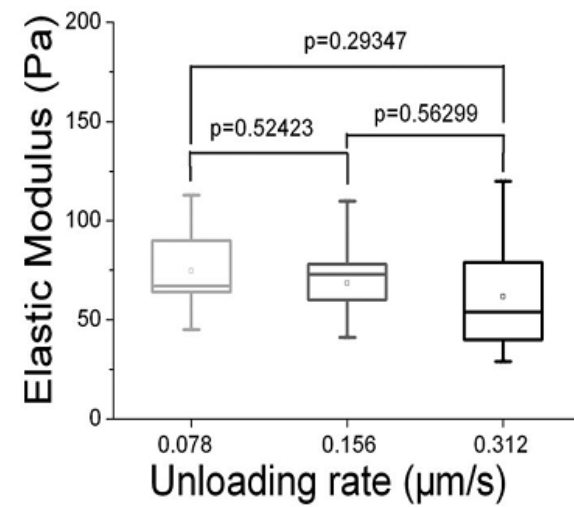
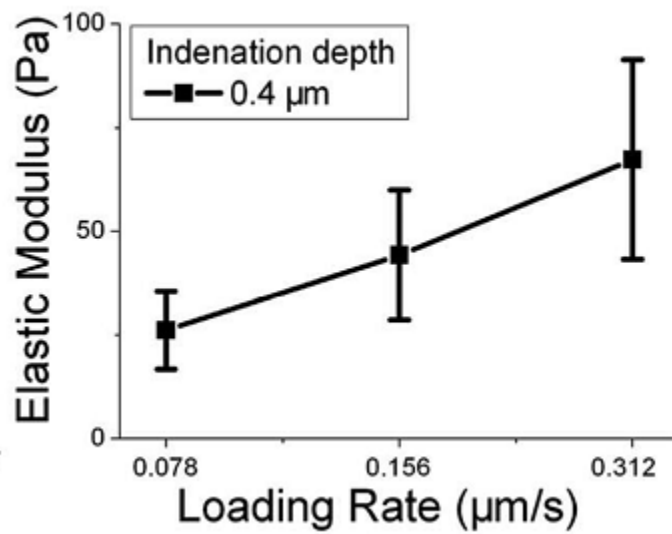


*rate-jump method for
Indentation-type AFM*

*J. Mech. Behav. Biomed.
Mater. 2007*

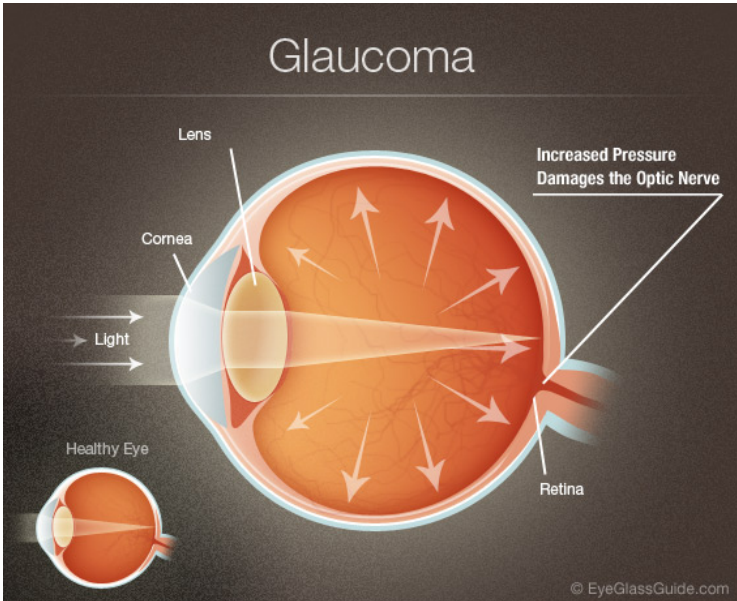


$$E_r = \frac{\dot{F}_u - \dot{F}_h}{2(\dot{h}_u - \dot{h}_h)\sqrt{R h_u}}$$



*rate-jump
method for
optical tweezers
indentation*

Case 1: Glaucoma Risk – Corneal Stiffness Investigated by Depth-sensing indentation

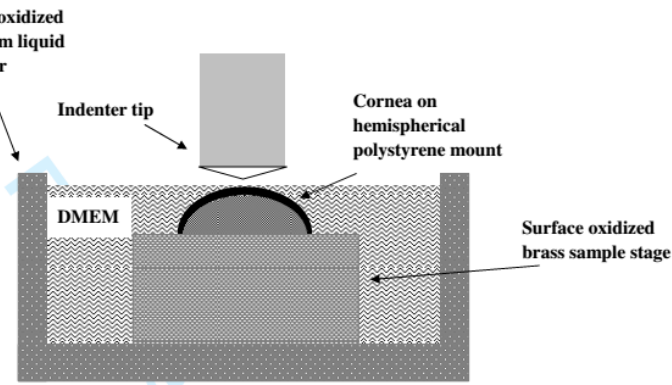


Objectives:

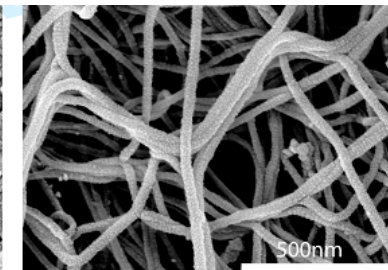
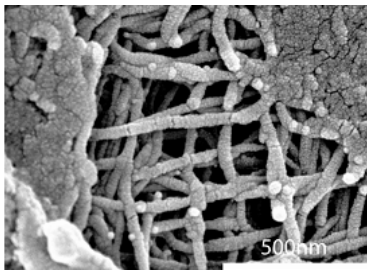
- Investigate the effects of IOP elevation on mechanical properties and microstructure of cornea *in vitro* in micron-scale
- Investigate the possibility of understanding glaucoma risk from the mechanical properties of cornea



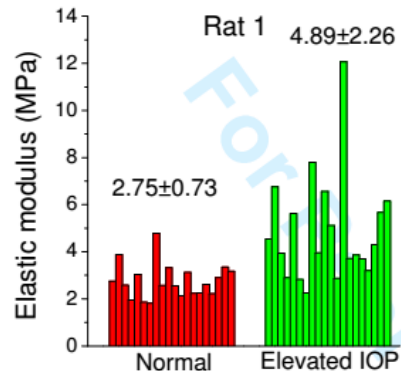
Soft Materials 2013



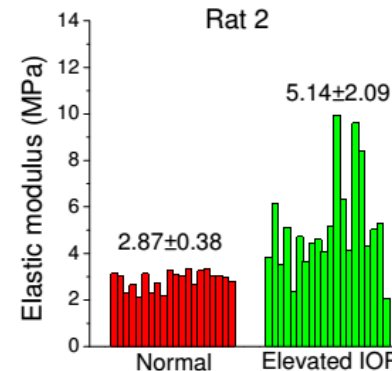
Liquid reservoir filled with distilled water



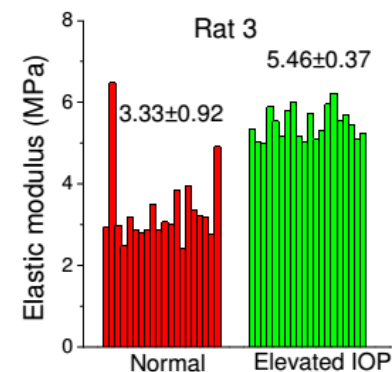
Tube system with valve connected to a standard 25g needle



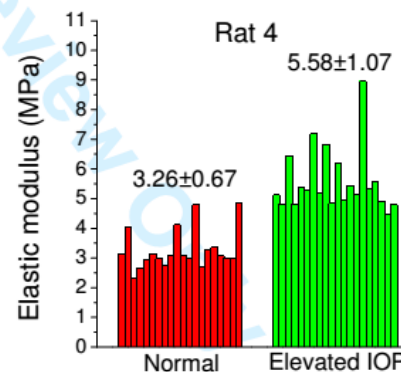
(a)



(b)

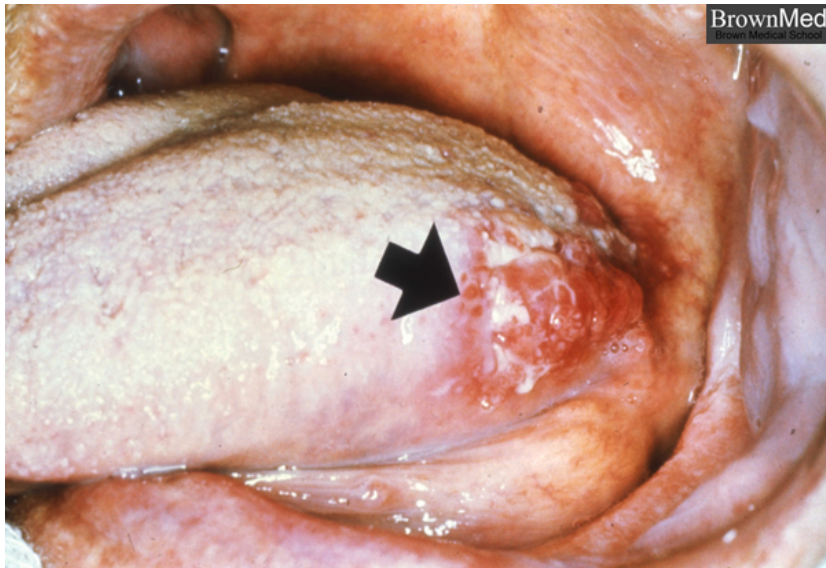


(c)

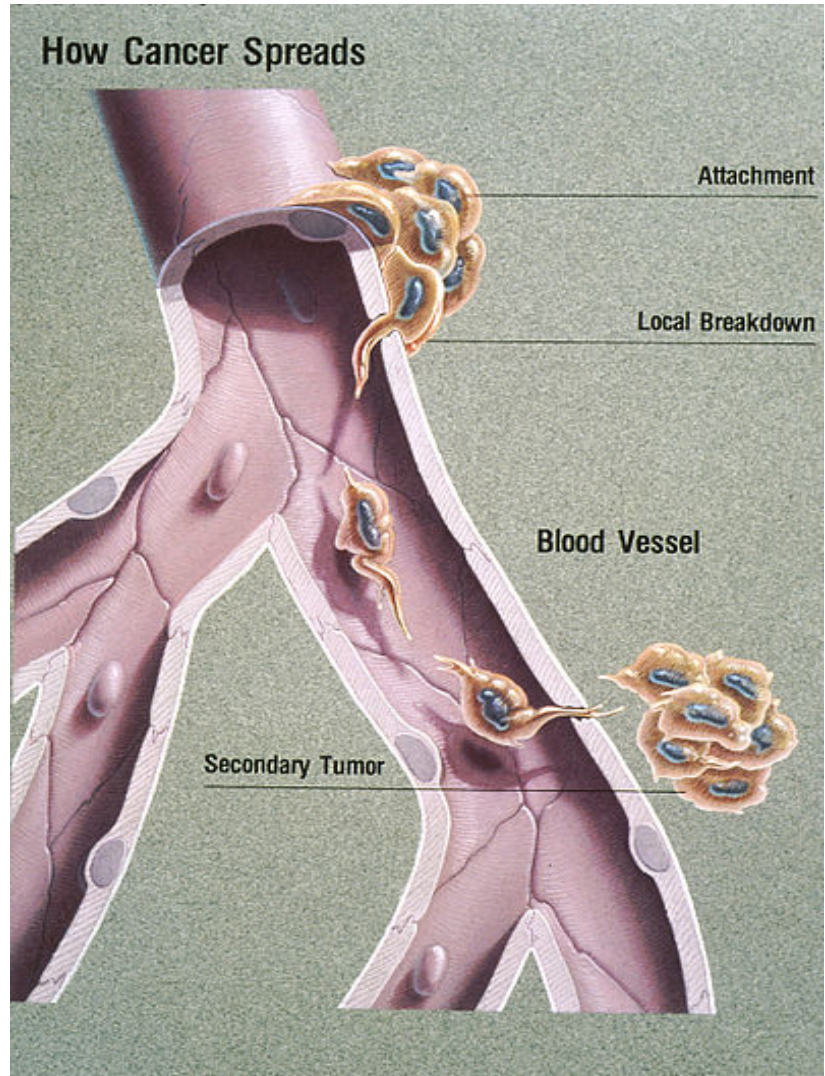


(d)

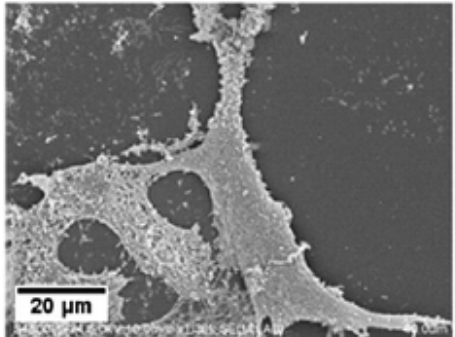
Case 2: Evaluation of Metastatic Potential of Tongue Squamous Carcinoma cells using IT-AFM



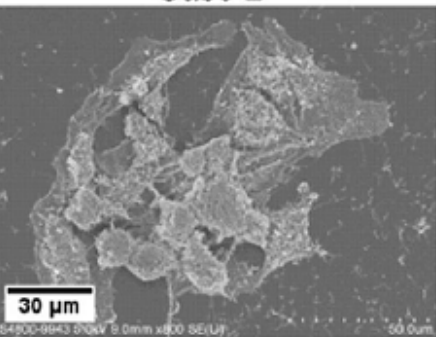
Determination of metastatic potential of tongue squamous cell carcinoma (TSCC) is very important in clinical treatment.



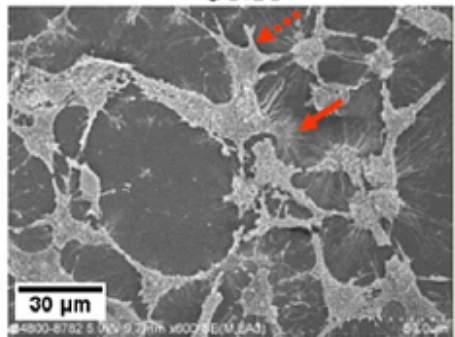
Case 1



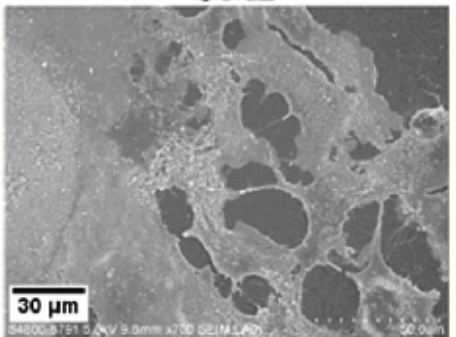
Case 2



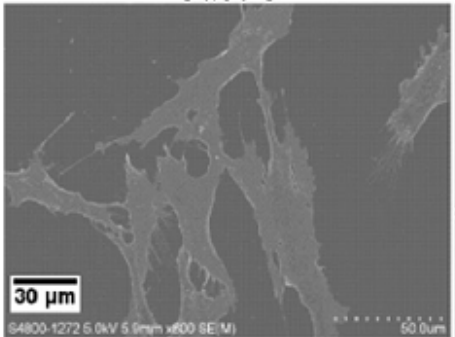
UM1



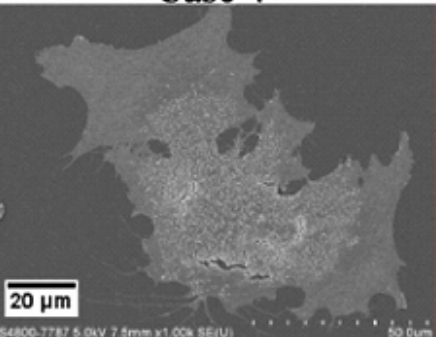
UM2



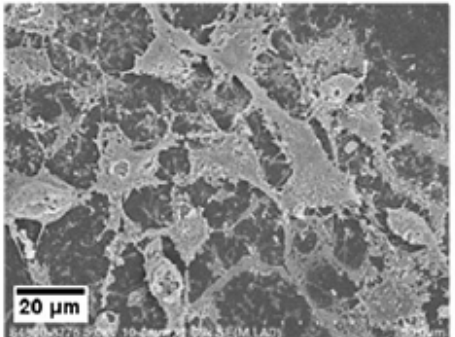
Case 3



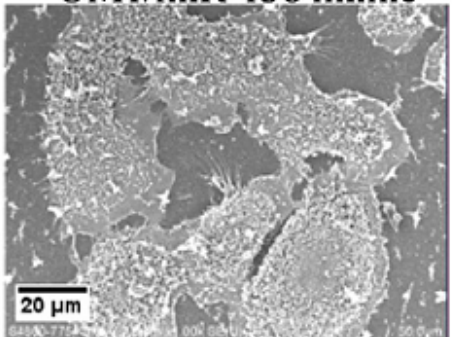
Case 4

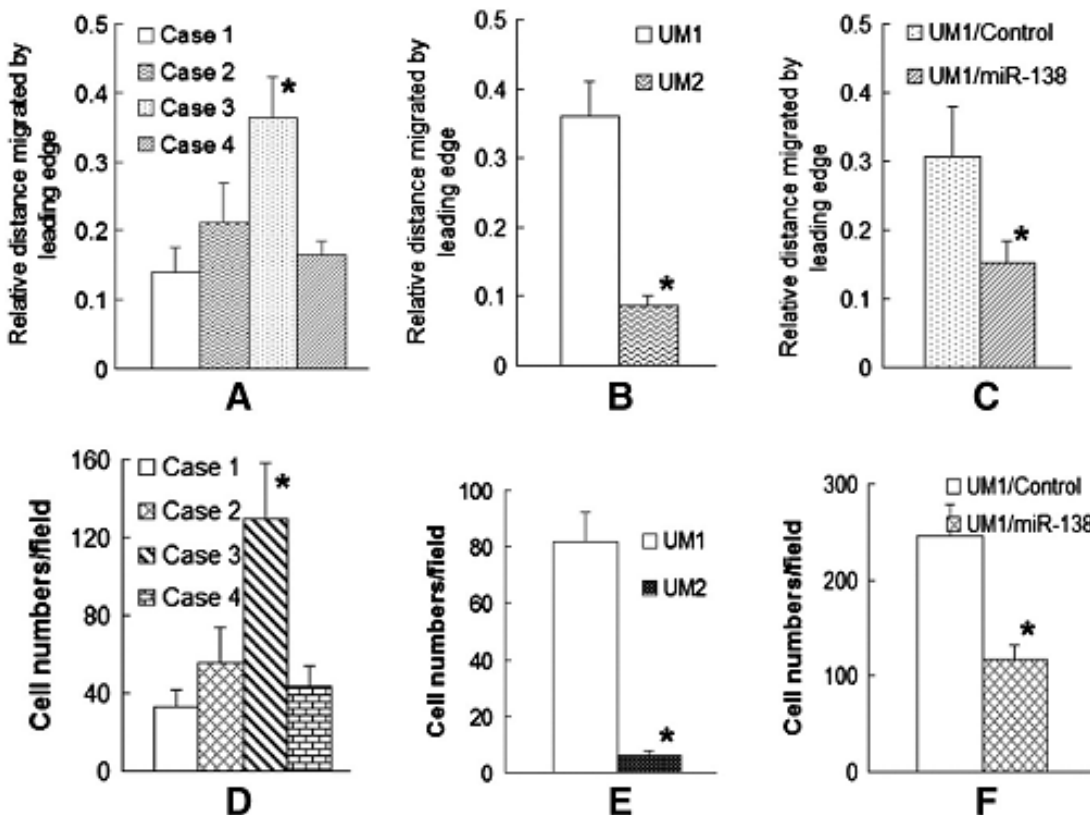


UM1/control mimic



UM1/miR-138 mimic



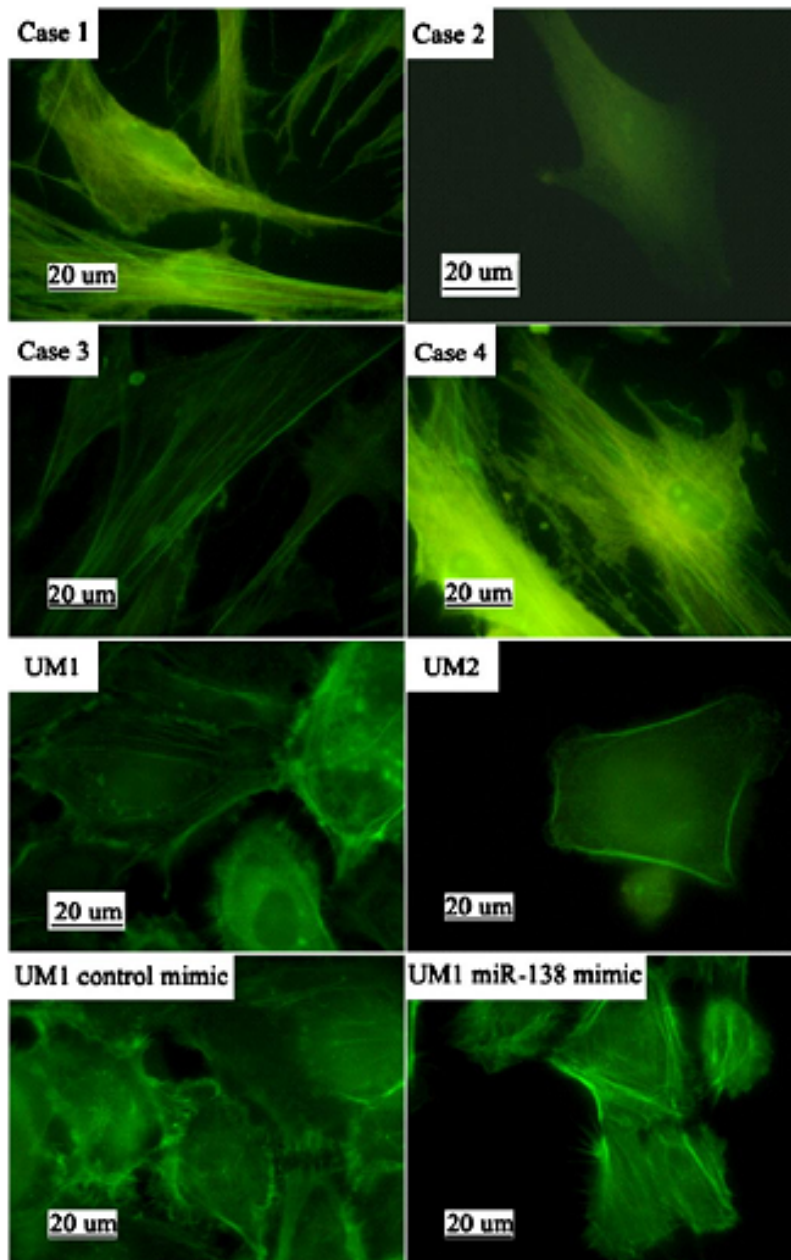


Metastatic potential of cells evaluate by wound-healing assay

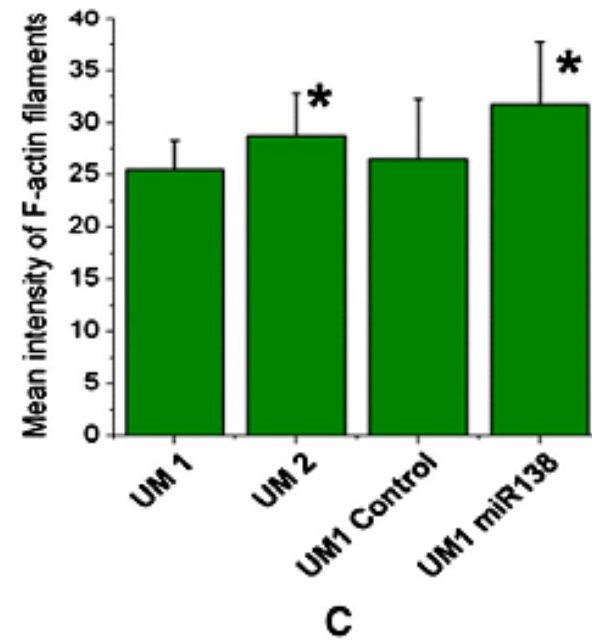
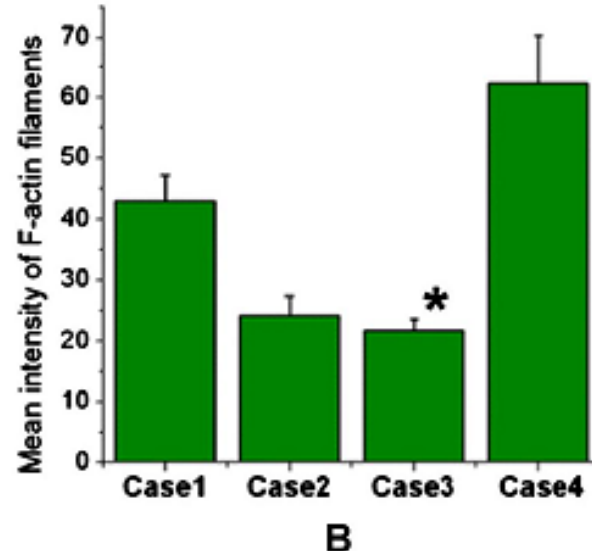
Elastic modulus value of TSCC cases and cell lines ($n = 30$).

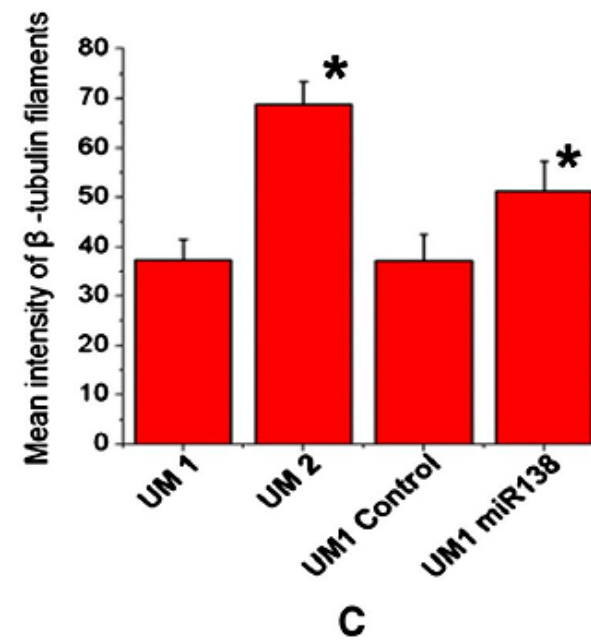
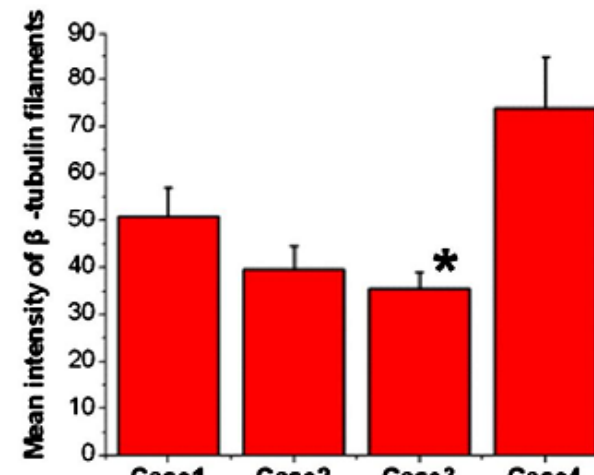
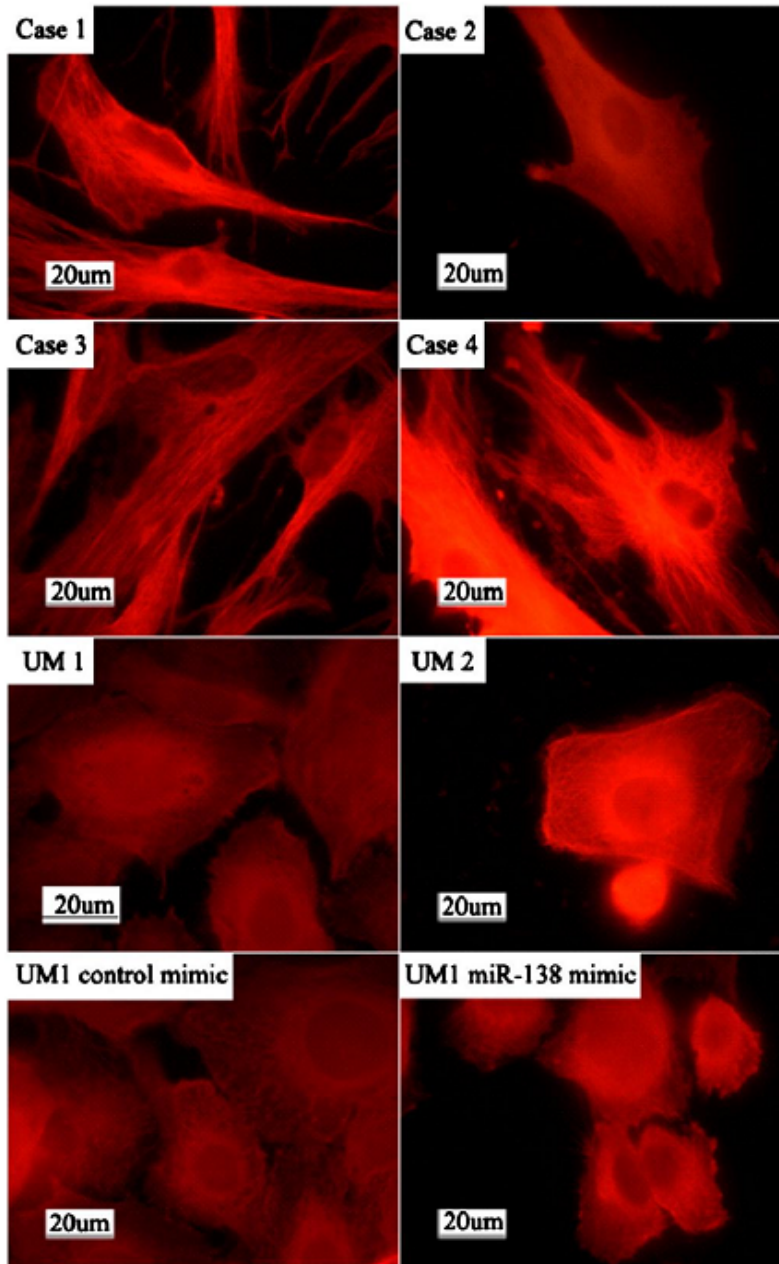
Cases	E_{elastic} (kPa)	Cell lines	E_{elastic} (kPa)
Case 1	7.55 ± 1.71	UM1	$3.65 \pm 1.01^*$
Case 2	4.92 ± 0.76	UM2	6.16 ± 1.39
Case 3	$4.09 \pm 0.72^*$	UM1/Control	$3.85 \pm 0.85^*$
Case 4	6.44 ± 1.13	UM1/miR-138	6.83 ± 1.65

The data are presented as mean \pm standard deviation. *: Case 3 compared with Case 1, Case 2, or Case 4; UM1 compared with UM2; UM1/Control compared with UM1/miR-138; $P < 0.05$.



A





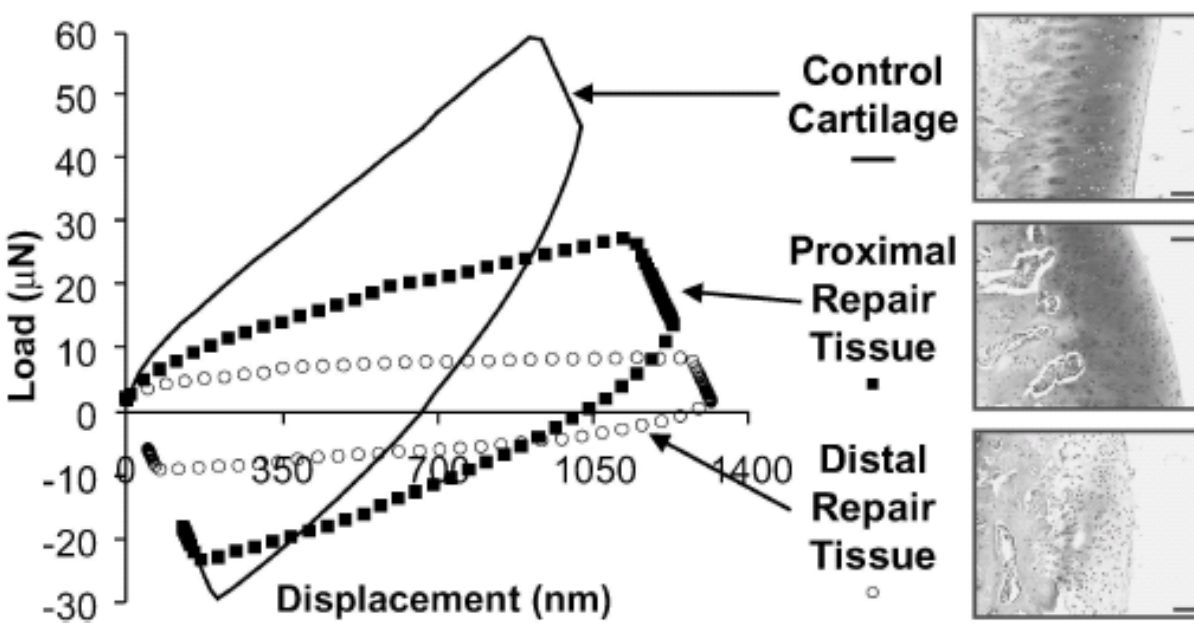
Cases	Nucleus size (μm^2)	N/C ratio
Case 1 (n = 60)	203.14 \pm 50.21	0.10 \pm 0.01
Case 2 (n = 54)	220.86 \pm 47.60	0.15 \pm 0.02
Case 3 (n = 46)	189.68 \pm 41.31*	0.20 \pm 0.03*
Case 4 (n = 51)	197.52 \pm 63.17	0.14 \pm 0.03

Cell lines	Nucleus size (μm^2)	N/C ratio
UM1 (n = 55)	207.24 \pm 57.79*	0.33 \pm 0.04*
UM2 (n = 51)	249.09 \pm 77.94	0.29 \pm 0.04
UM1/Control (n = 100)	203.58 \pm 53.42*	0.32 \pm 0.05*
UM1/miR-138 (n = 50)	213.13 \pm 47.6	0.26 \pm 0.04

Elastic modulus value of TSCC cases and cell lines (n = 30).

Cases	E_{elastic} (kPa)	Cell lines	E_{elastic} (kPa)
Case 1	7.55 \pm 1.71	UM1	3.65 \pm 1.01*
Case 2	4.92 \pm 0.76	UM2	6.16 \pm 1.39
Case 3	4.09 \pm 0.72*	UM1/Control	3.85 \pm 0.85*
Case 4	6.44 \pm 1.13	UM1/miR-138	6.83 \pm 1.65

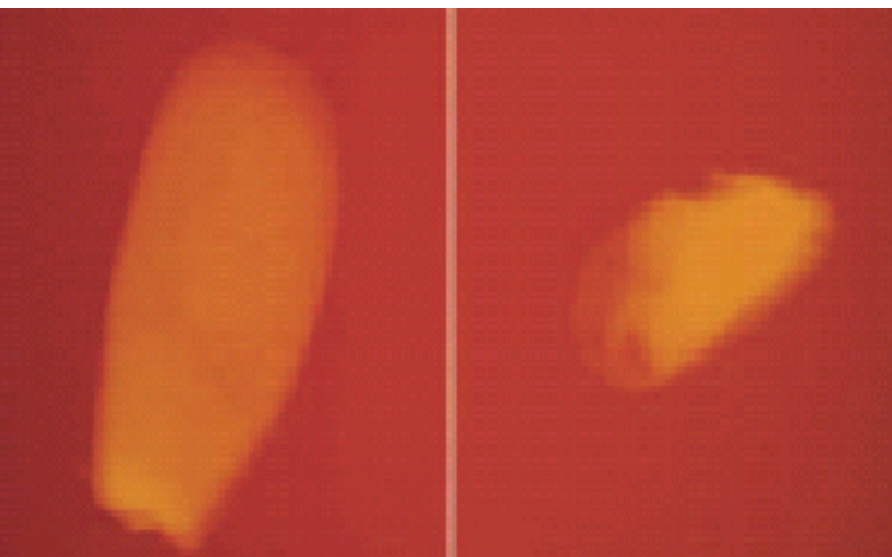
The data are presented as mean \pm standard deviation. *: Case 3 compared with Case 1, Case 2, or Case 4; UM1 compared with UM2; UM1/Control compared with UM1/miR-138; $P < 0.05$.



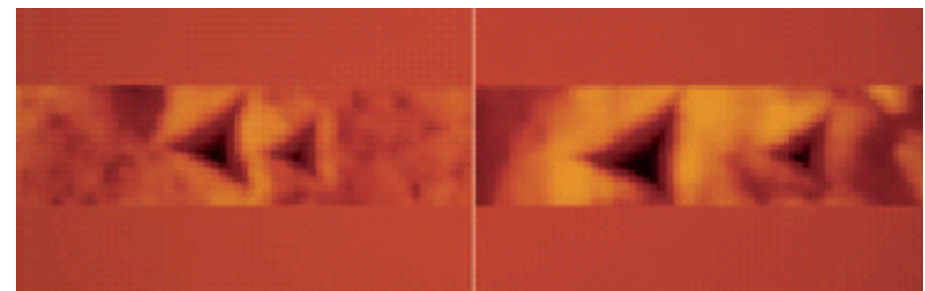
Are the mechanical properties measured accurate?

Ebenstein et al., 2004, Journal of Materials Research

Nanoindentation tests to measure the mechanical properties of cartilage repair tissue in rabbit knees.



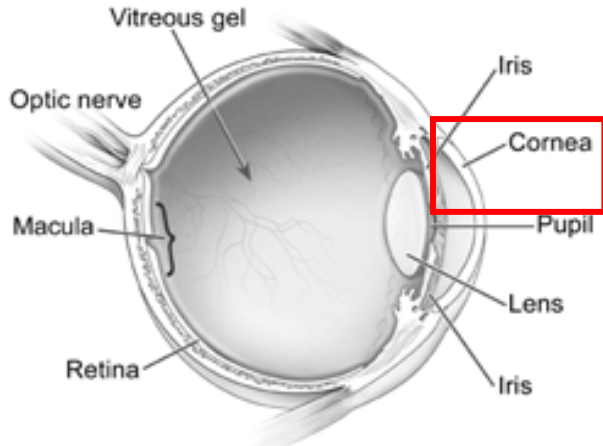
Images of bovine and human sperm nuclei.



Indentations on bovine and human sperm nuclei.

<http://www.veeco.com/>

Case 1: Glaucoma Risk - Stiffness of Cornea in relation to Intraocular Pressure (IOP) Investigated by Depth-sensing indentation



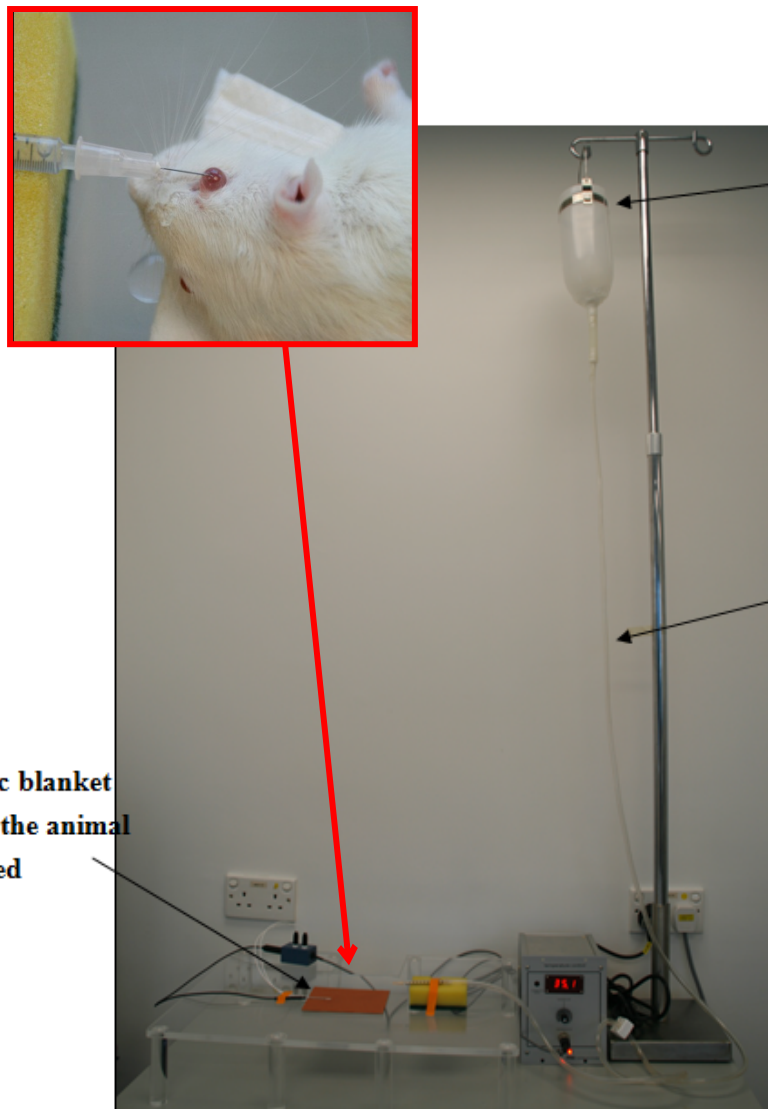
Objectives:

- Investigate the effects of IOP elevation on mechanical properties and microstructure of cornea *in vitro* in nano-scale
- Investigate the possibility of understanding glaucoma risk from the mechanical properties of cornea

Animal Model:

- Adult male SD-Rats
- Weight: 250g-290g
- Corneas stored in BSS solution immediately after harvested
- DmEm used to simulate *in vivo* conditions

Method to increase IOP acutely *in vivo*:



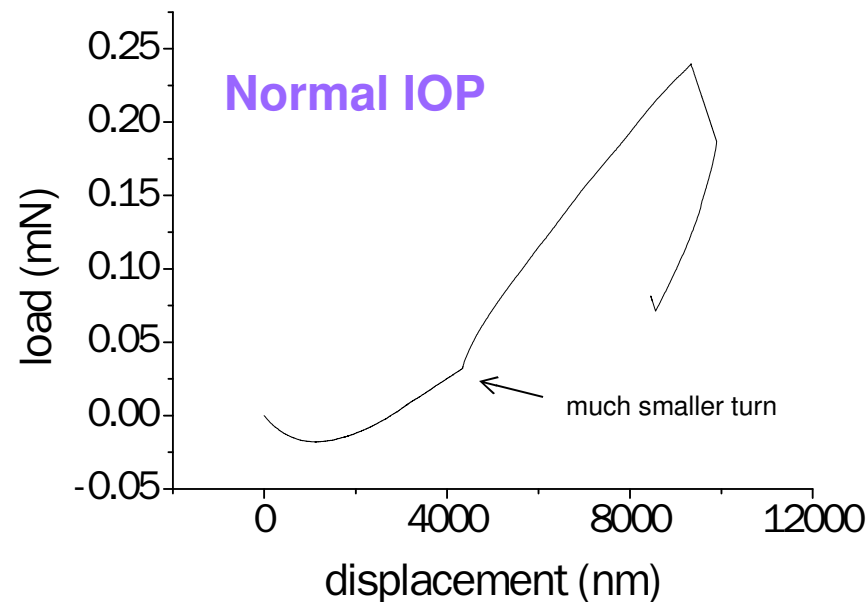
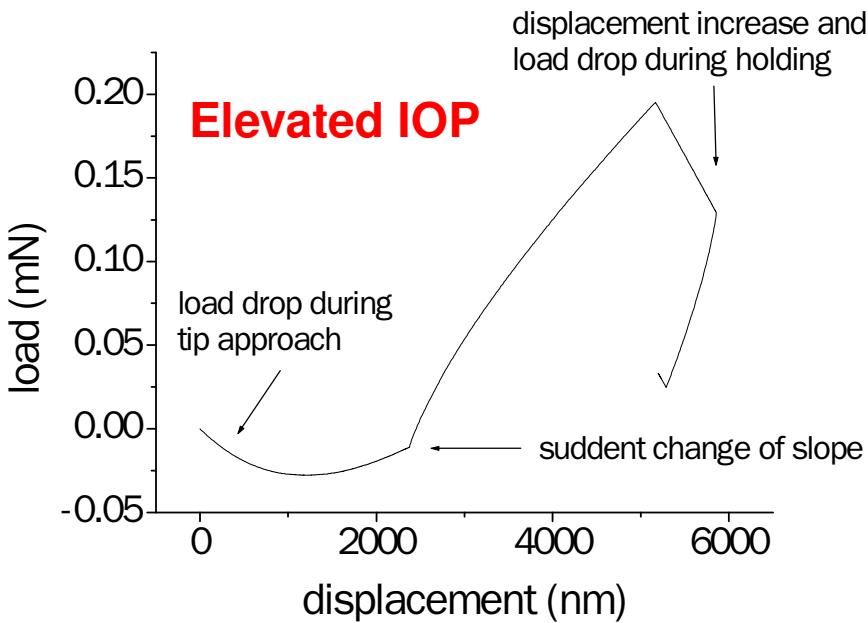
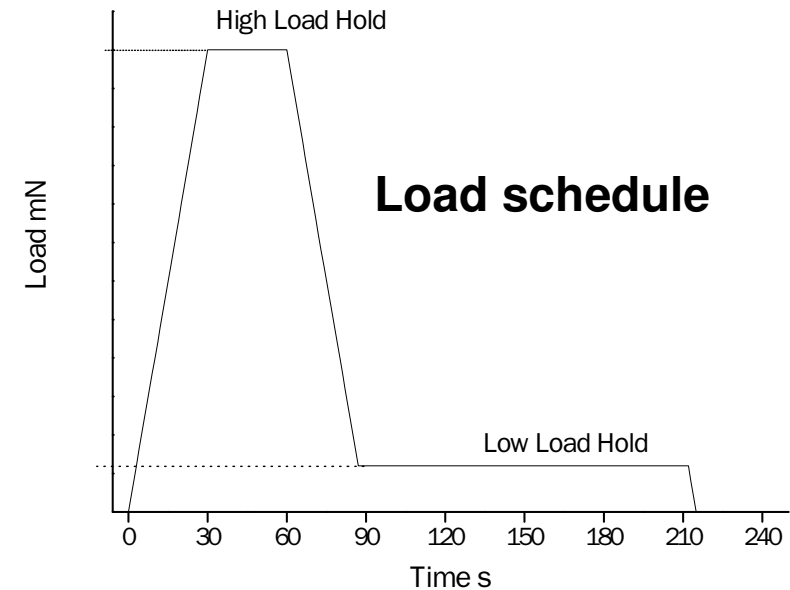
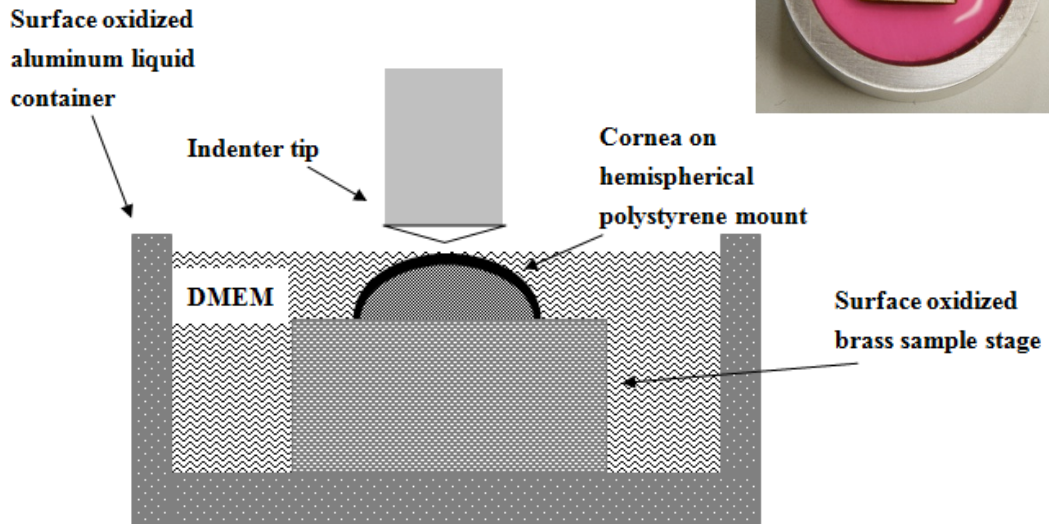
- Rat anesthetized and fixed on the operating table

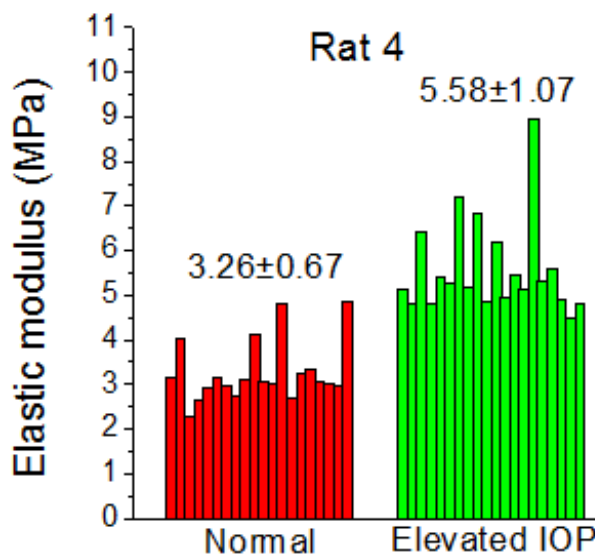
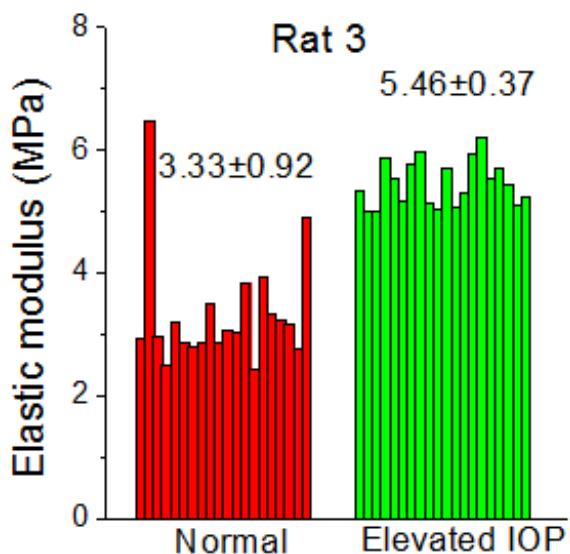
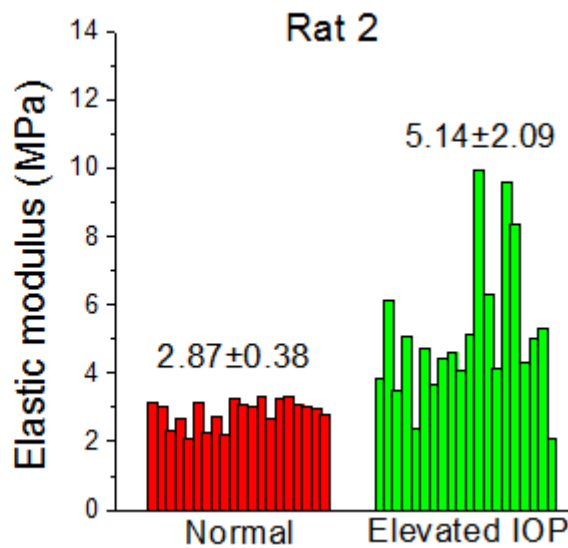
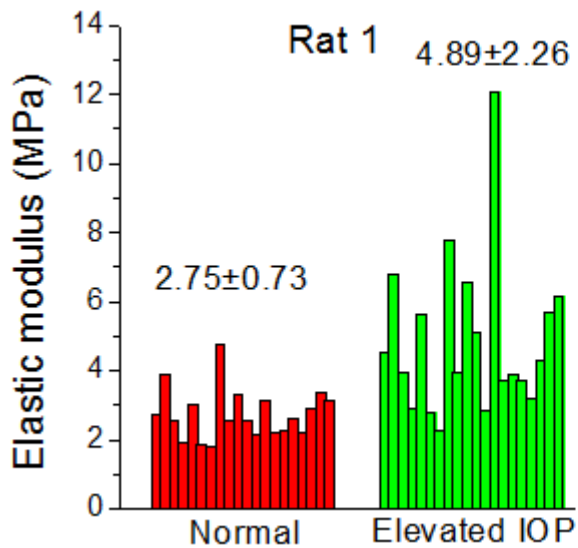
- Right eyeball connected to the liquid reservoir by a needle, subjected to IOP elevation of 120 mmHg (c.f. normal IOP 10-20 mmHg)

- Duration: 1 hour and the rat was injected every 15 minutes to ensure it was anesthetized

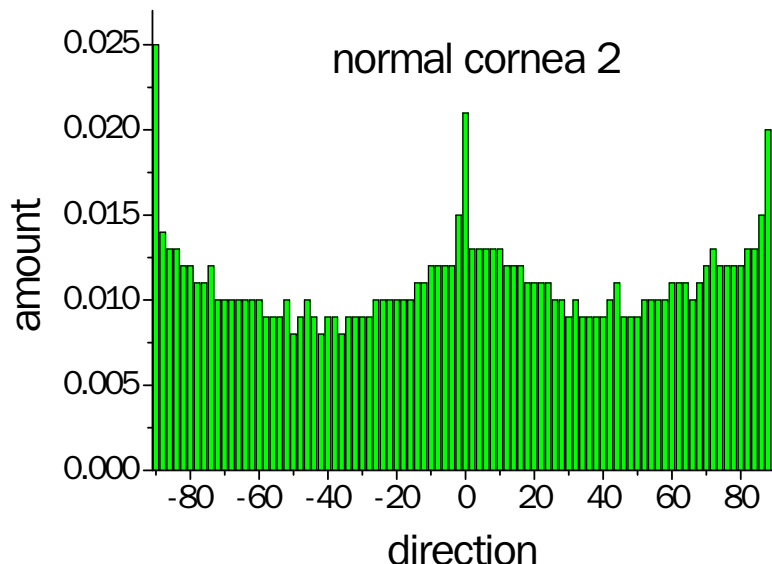
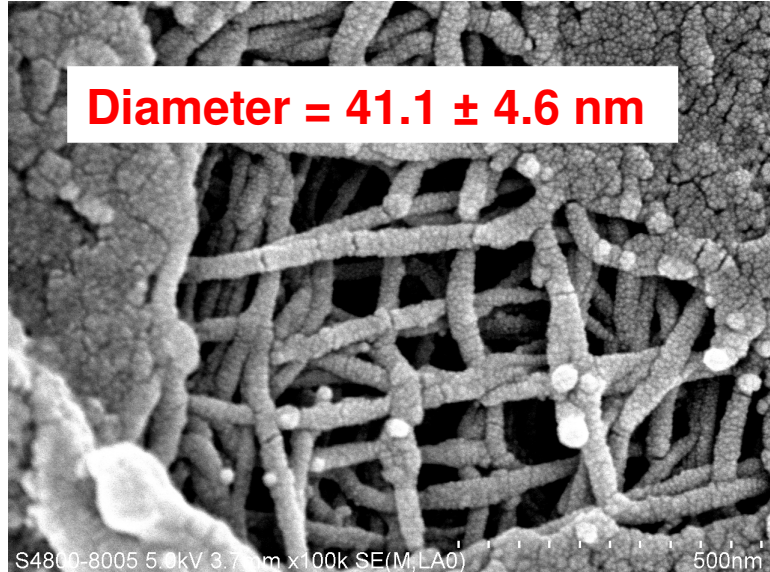
- Cornea stored in BSS solution and refrigerated

Nanoindentation

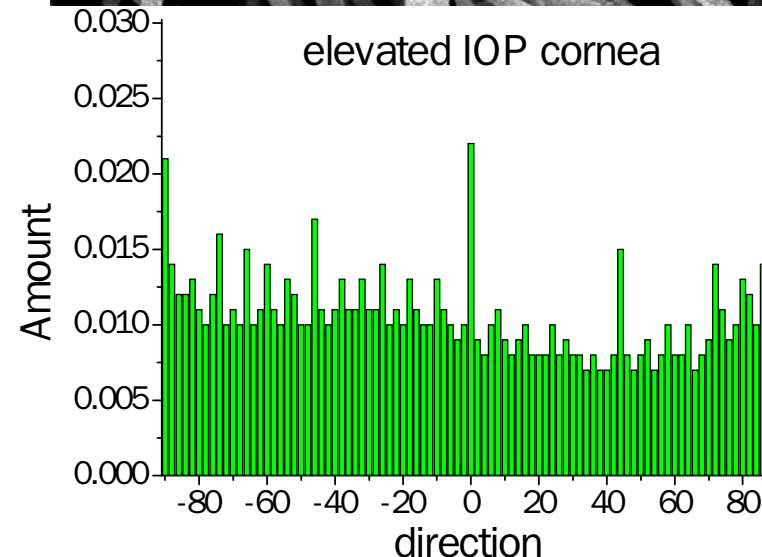
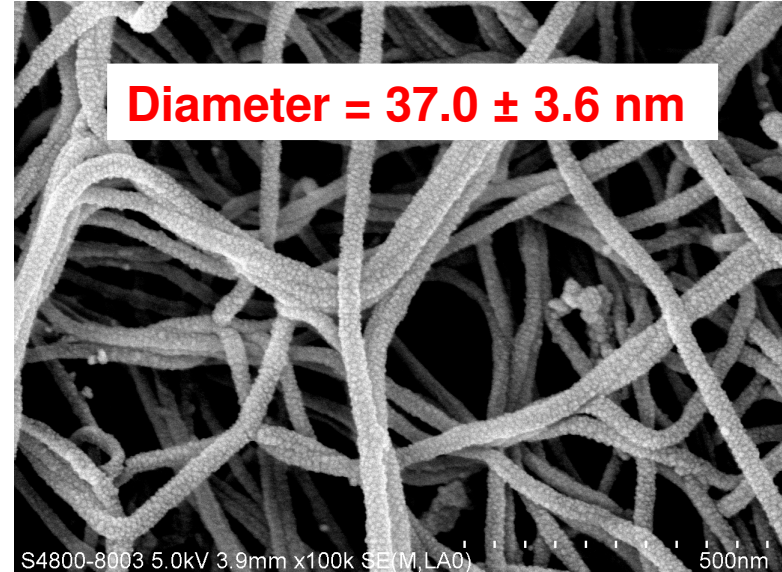




SEM of Collagen Fibrils in Cornea (after load removal and critical-point drying)



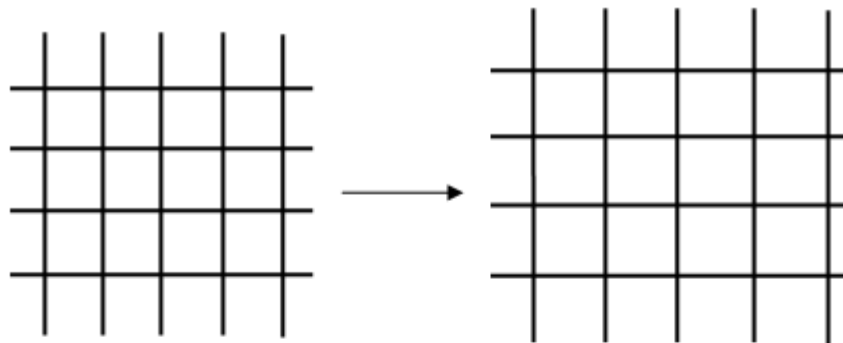
Normal IOP



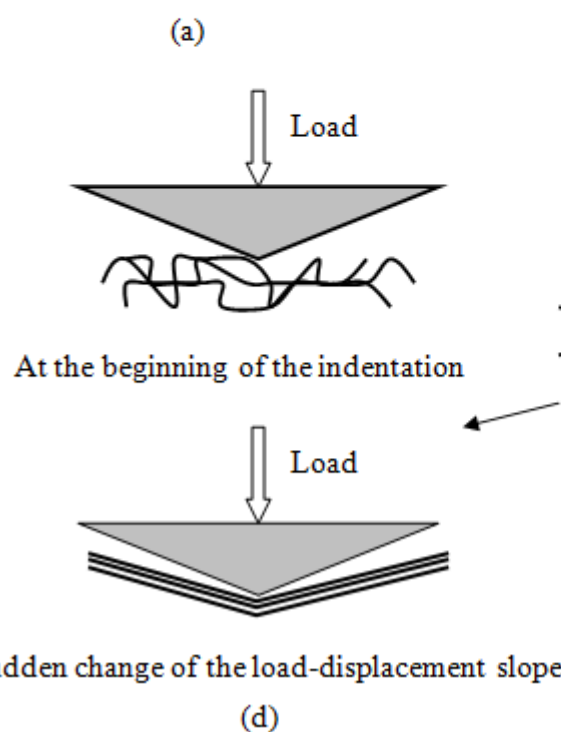
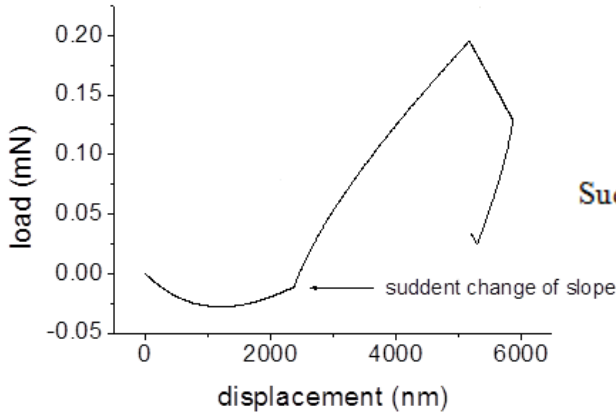
Elevated IOP

Possible Events

Original regular collagen fiber network



Loosened collagen fibrils becoming taut during indentation, resulting in a change of slope in the load-displacement curve.



Collagen fiber network under elevated IOP

Relaxed collagen fiber network after removal of elevated IOP

Conclusions:

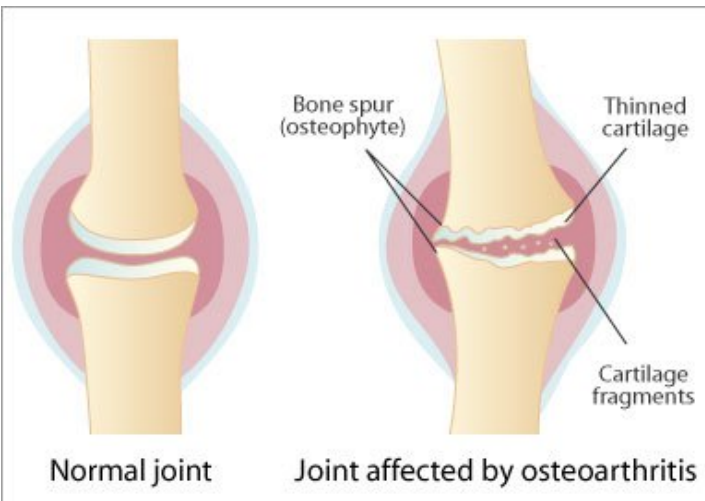
Elevated IOP of 120 mmHg (~10 times higher than normal) in SD-rats over 1 hour increases elastic modulus of cornea by 2.1 to 2.4 MPa (c.f. normal value of ~3 MPa).

The elevated IOP thins down the collagen fibrils, from about 41 to 37 nm. Substantial relaxation of the fibril network happens upon load removal.

Case 2: Low Compliance of Individual Collagen Fibrils in Osteoarthritic Cartilage of Human Beings Revealed by Atomic Force Microscopy

Objectives:

To investigate the mechanical properties of individual collagen fibrils of articular cartilage (AC) harvested from patients suffered from osteoarthritis (OA) by AFM nanoindentation, therefore try to figure out the possibility to use the change of nanomechanical properties of individual collagen fibrils as the indicator for early detection of OA.



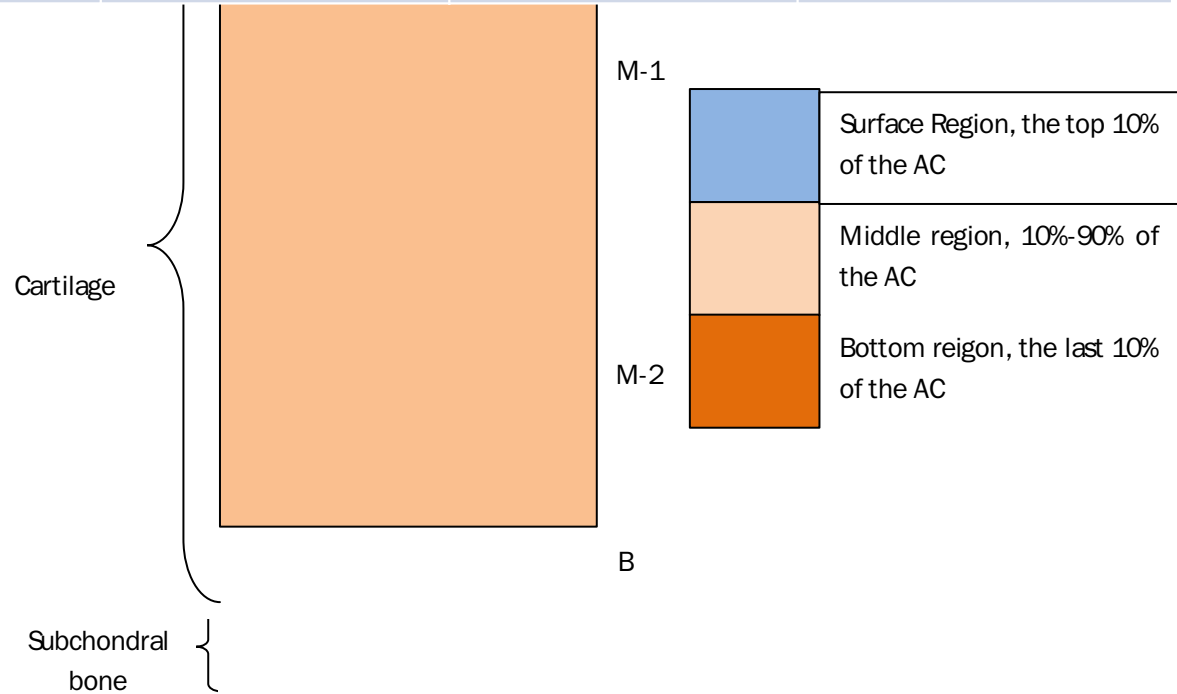
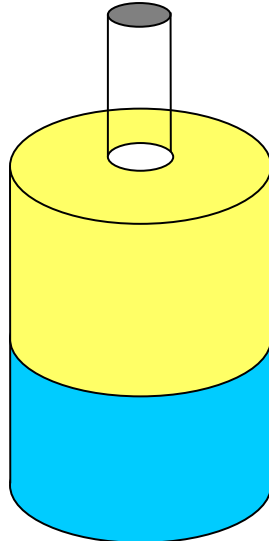
Detailed information of specimens

Specimens	OP (n=20)	OA-1 (n=20)	OA-2 (n=18)	OA-3 (n=18)
Age/sex	F/60	F/59	F/52	F/70
Diagnosis	Hip fracture	OA Knee	OA knee	OA-hip
Thickness	4.0 mm	3.5 mm	2.3 mm	1.5 mm

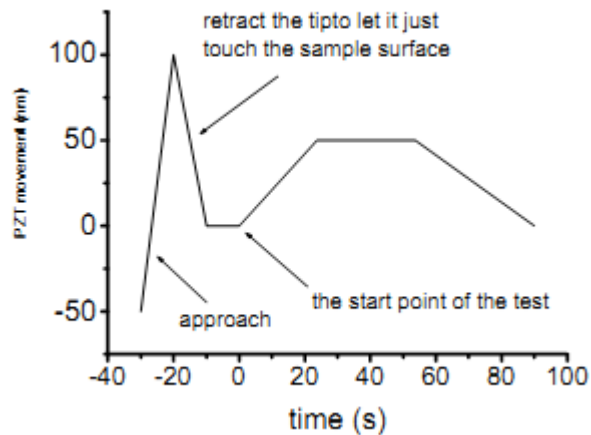
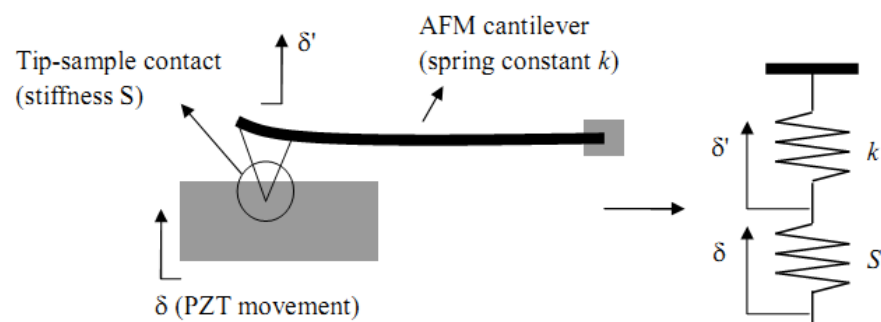
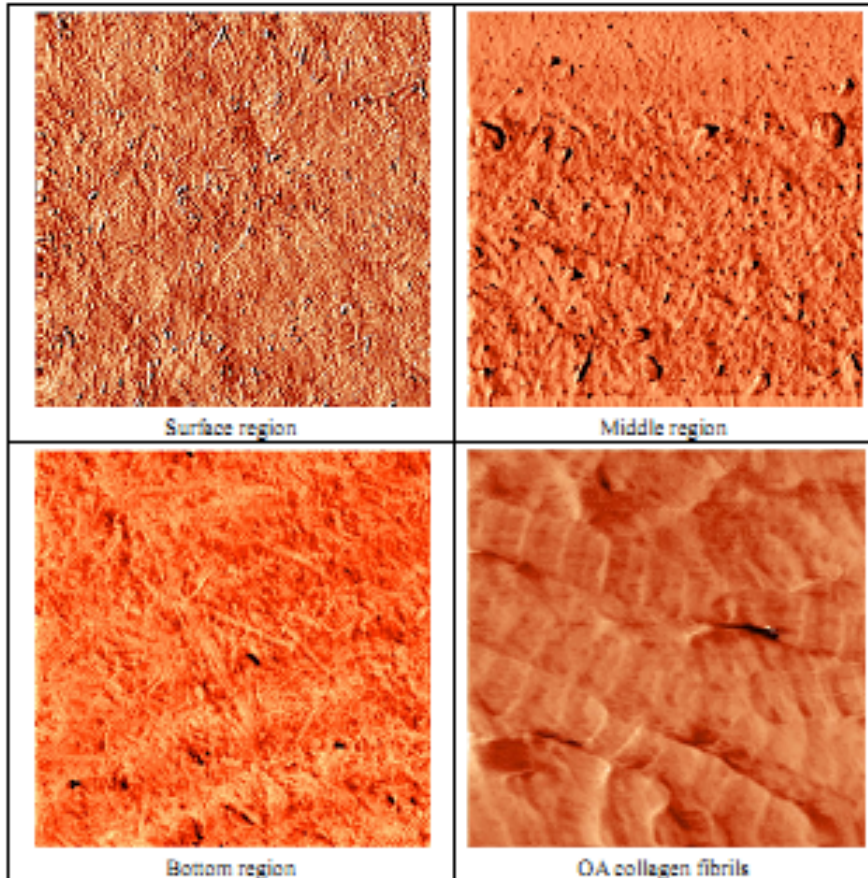
cartilage was harvested by punch

articular cartilage

subchondral bone

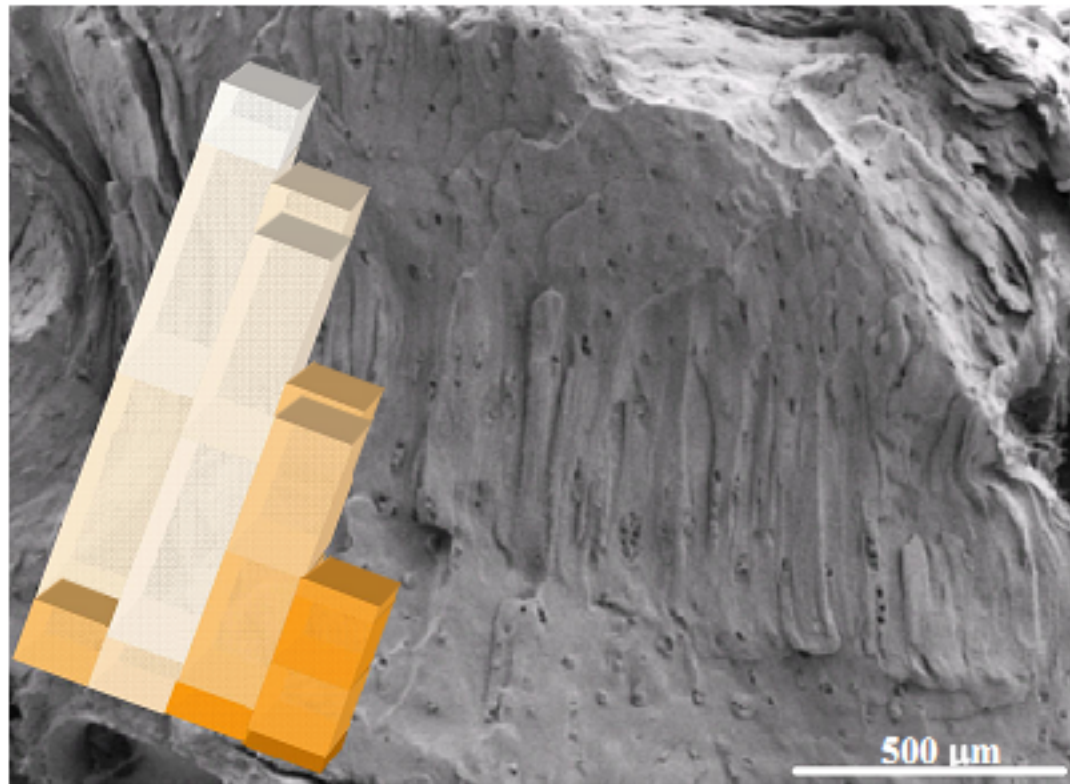


AFM nanoindentation



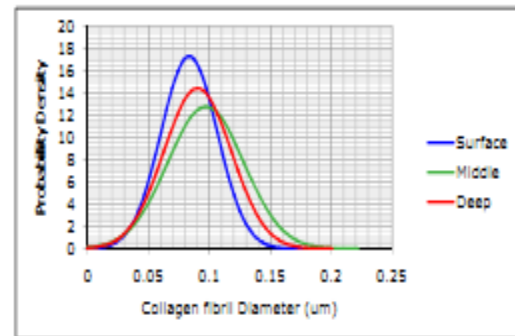
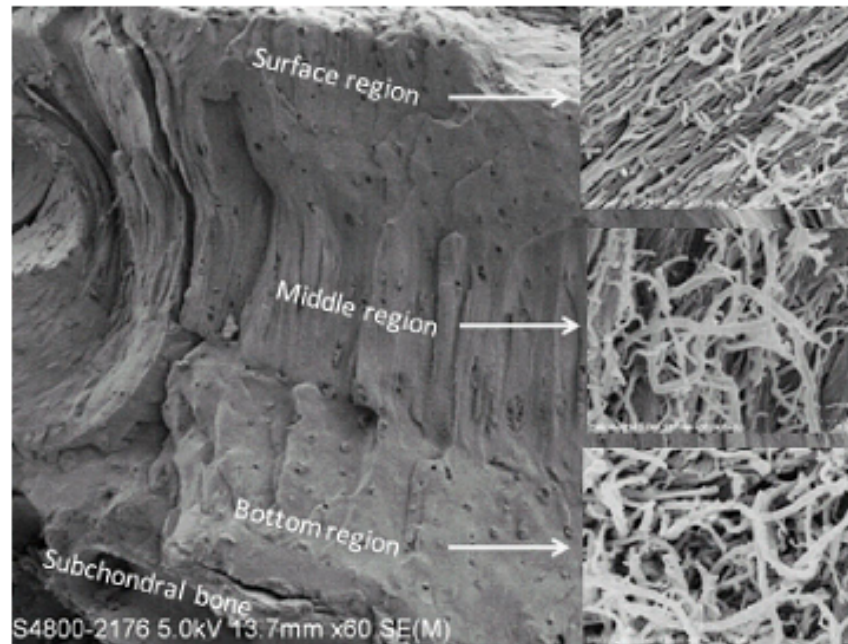
Typical AFM images ($5 \times 5 \mu\text{m}$) of AC samples (a-c) and scanned collagen fibrils at high magnification($1 \times 1 \mu\text{m}$)

	Elastic modulus (GPa), Mean±S.E.M, the Possion's Ratio was taken to be			
Specimens	OP (n=20)	OA-1 (n=20)	OA-2 (n=18)	OA-3 (n=18)
S	2.06±0.31	2.38±0.18	3.01±0.14	3.56 ± 0.18
M-1	2.20±0.14	2.27±0.15	2.82±0.12	3.69 ± 0.19
M-2	2.38±0.14	2.23±0.12	3.05±0.25	3.58 ± 0.24
B	3.13±0.21	2.55±0.12	3.79±0.22	4.36 ± 0.23

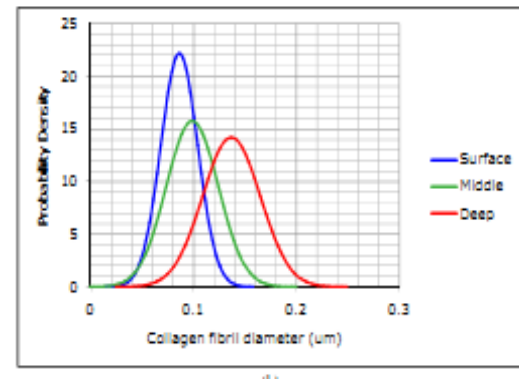


- the elastic modulus of individual collagen fibrils increase gradually from the surface region to the bottom region
- individual collagen fibrils at the surface and the bottom became stiffer with the progressing of OA

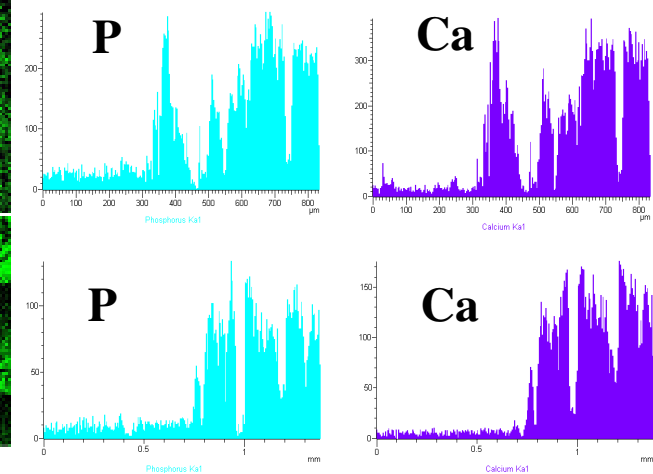
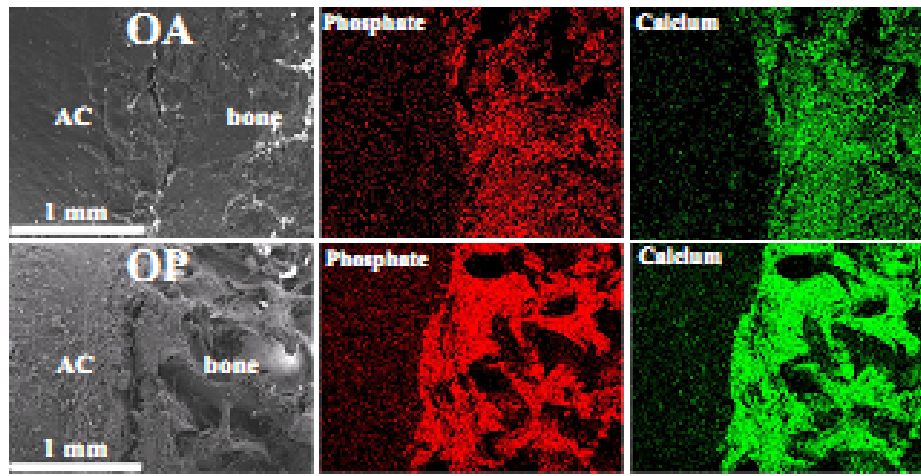
SEM study



(a)



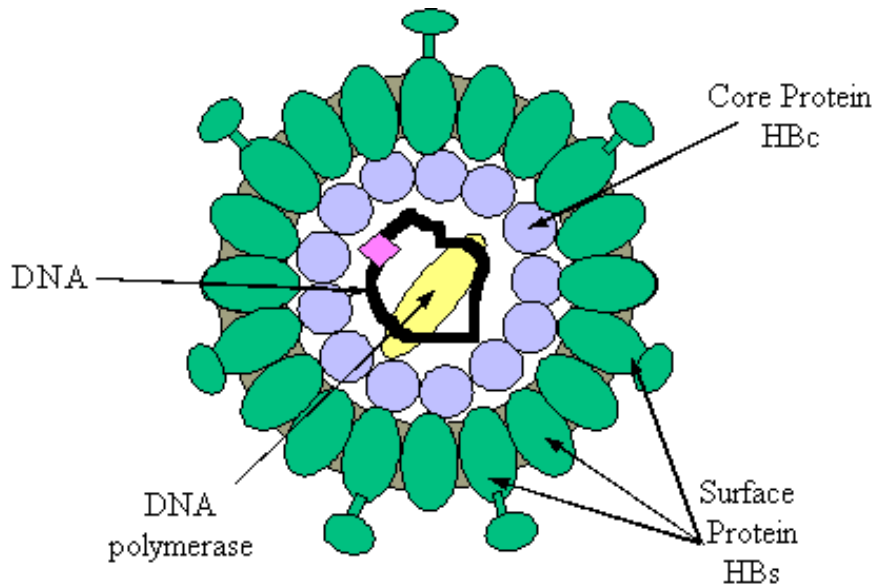
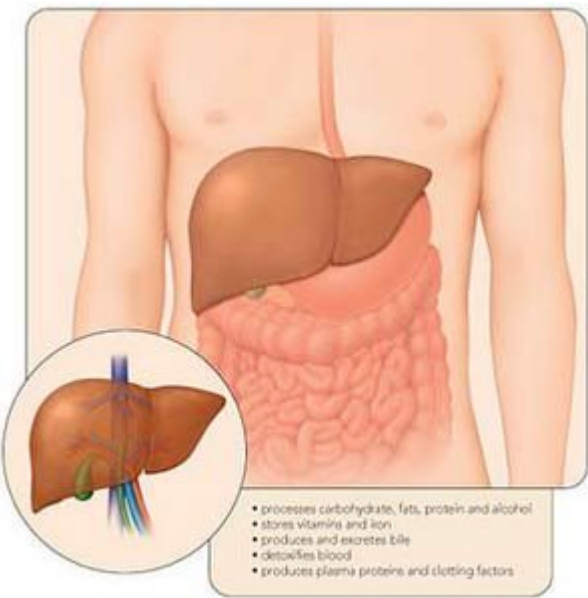
(b)



Conclusions:

- In the normal cartilage, stiffness of the collagen fibrils increase gradually from the surface part to the bone part
- The individual collagen fibrils's elastic modulus increase significantly with the progressing of OA, which can possiblly to be used as a indicator for OA monitoring and diagnosis.

Case 3: Hepatitis B Surface Antigen-antibody Interactions Studied by Optical Tweezers



Fact about Hepatitis B :

- serious disease that affects the liver
- About 2 billion people worldwide have been infected with the virus
- 600,000 persons die per year
- production of highly sensitive, antibodies for HBV detection is critical in clinical treatment

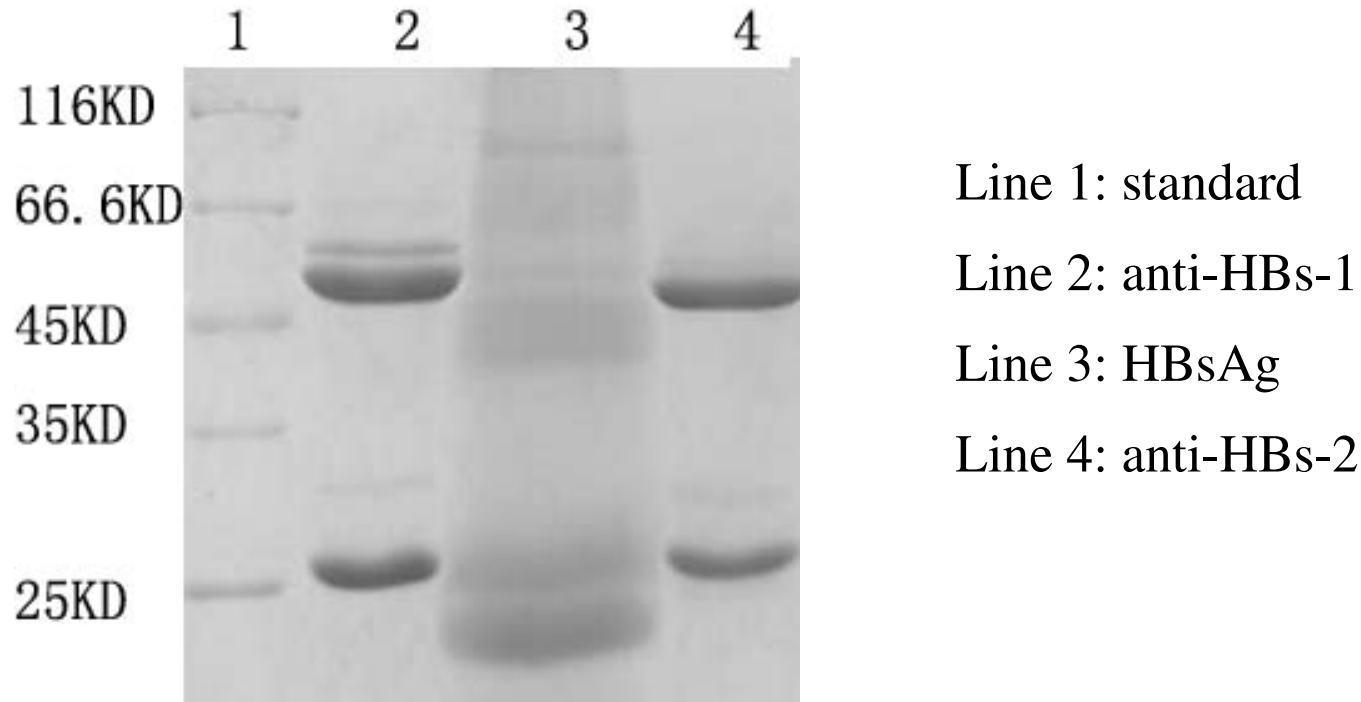
Experimental details

Antigen and antibodies

Hepatitis B Surface Antigen (HBsAg) - supplied by Shanghai Genomintel (China)

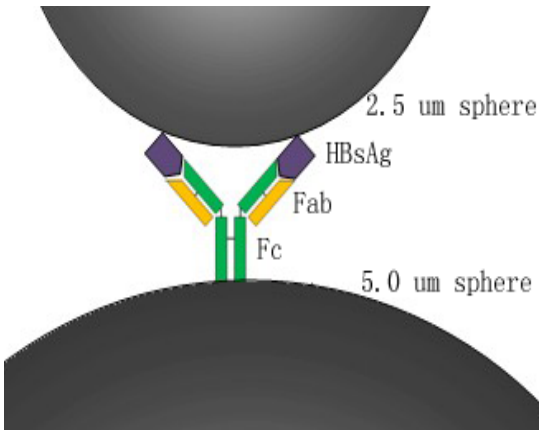
Hepatitis B Surface Antibody 1 (Anti-HBs-1)- Daangene company (China)

Hepatitis B Surface Antibody 2 (Anti-HBs-2)- Shanghai QcBio (China)



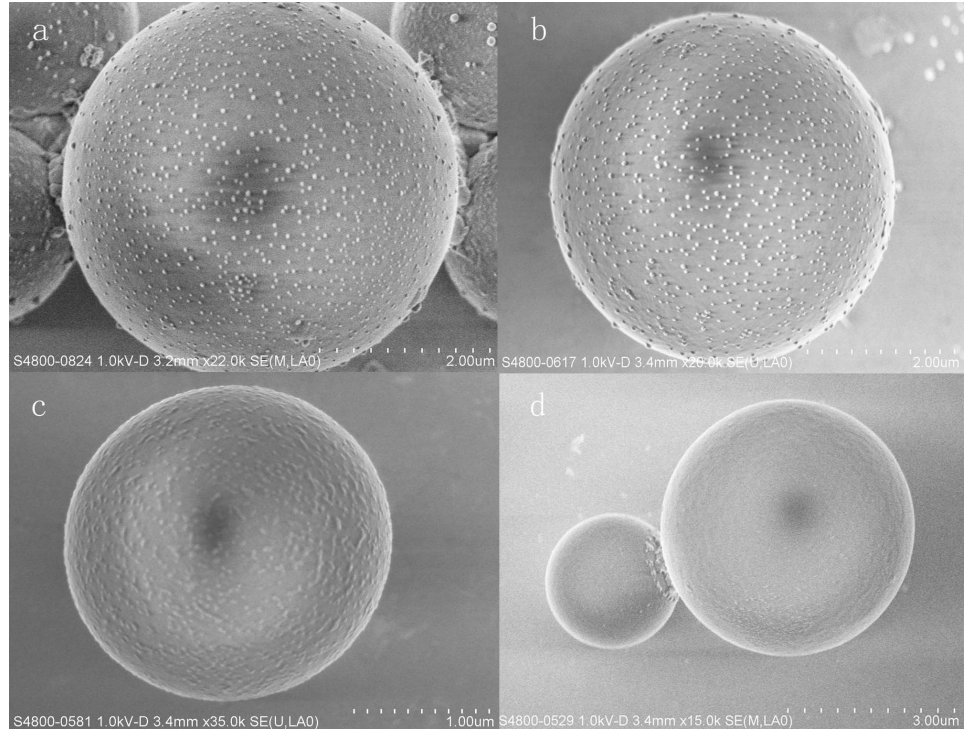
Coomassie blue stained SDS-PAGE pattern of HBsAg and anti-HBs

Microsphere coating procedure



Hydrophobic bonding
between the Fc segment of
anti-HBs

- Overdose of HBsAg were added
- Hydrophobic bonding between anti-HBs and microsphere surface enhance the antigen-antibody interaction
- Uncoated surface was sealed with BSA

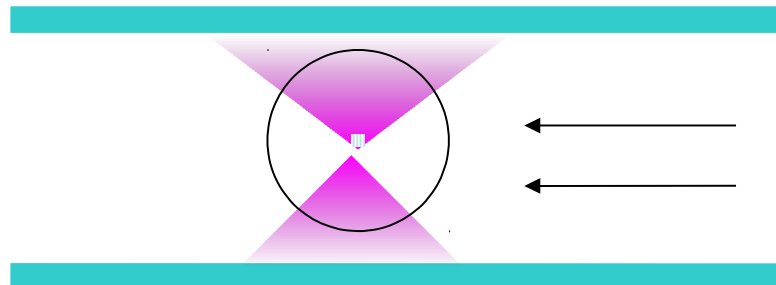


SEM images of different protein-coated and uncoated microspheres. (a) anti-HBs-1 proteins coated on a 5 mm PS microsphere, (b) anti-HBs-2 proteins coated on a 5 mm PS microsphere, (c) HBsAg proteins coated on a 2.5 mm PS microsphere, (d) uncoated 2.5 mm and 5 mm PS microspheres.

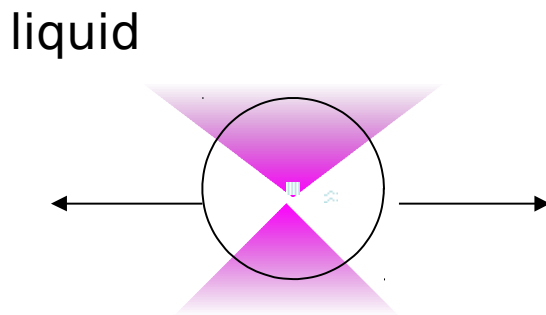
Force calibration of optical tweezers

Key equation:

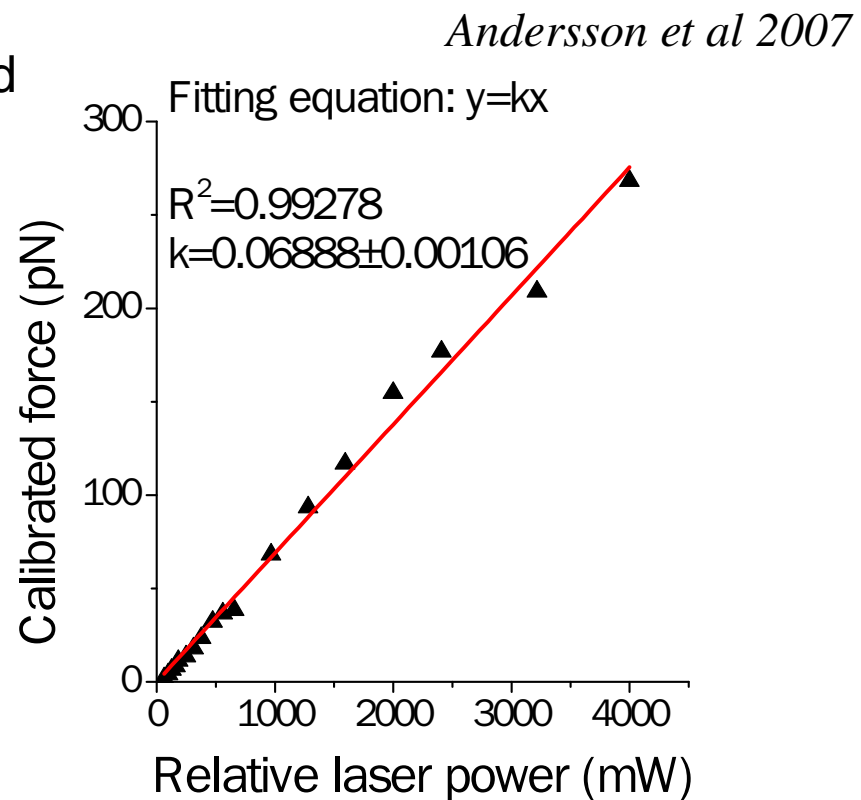
$$F_{\max}(x, t) = 6\pi^2 \eta a A_c \omega$$

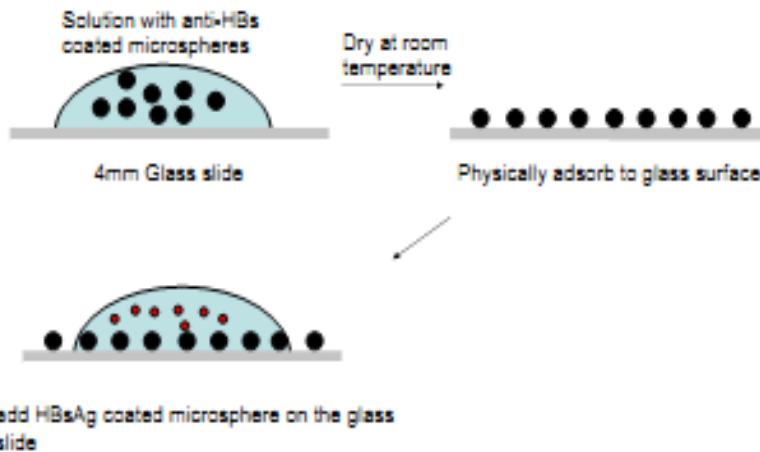


Traditional method



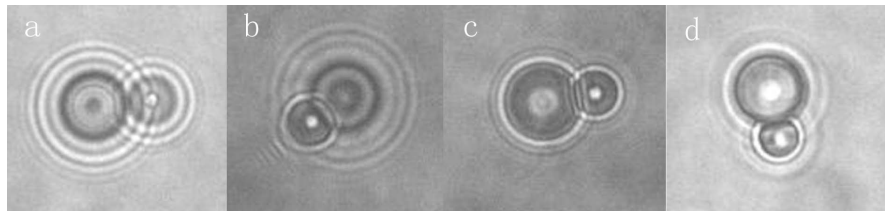
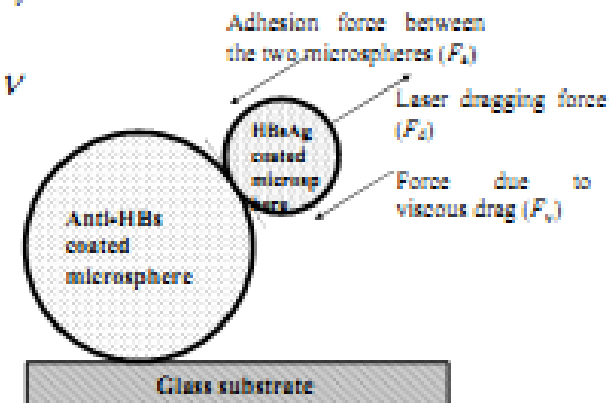
Calibration method in our
optical tweezers



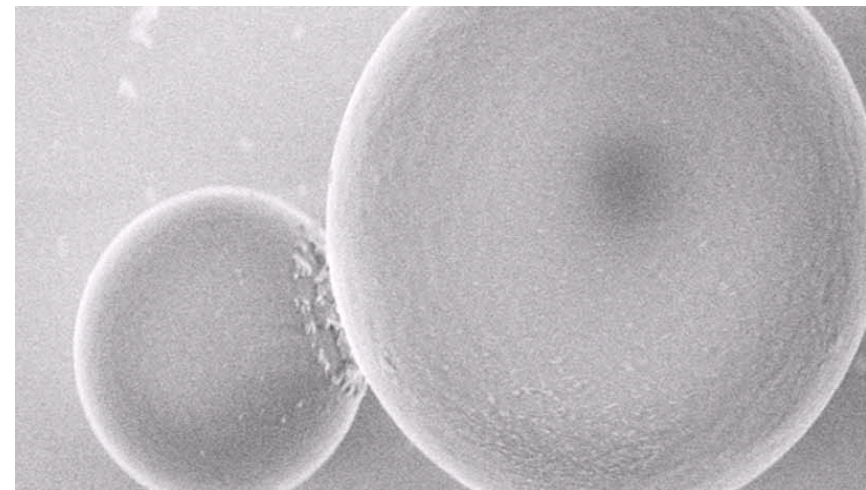


$$F_a = F_d - F_v$$

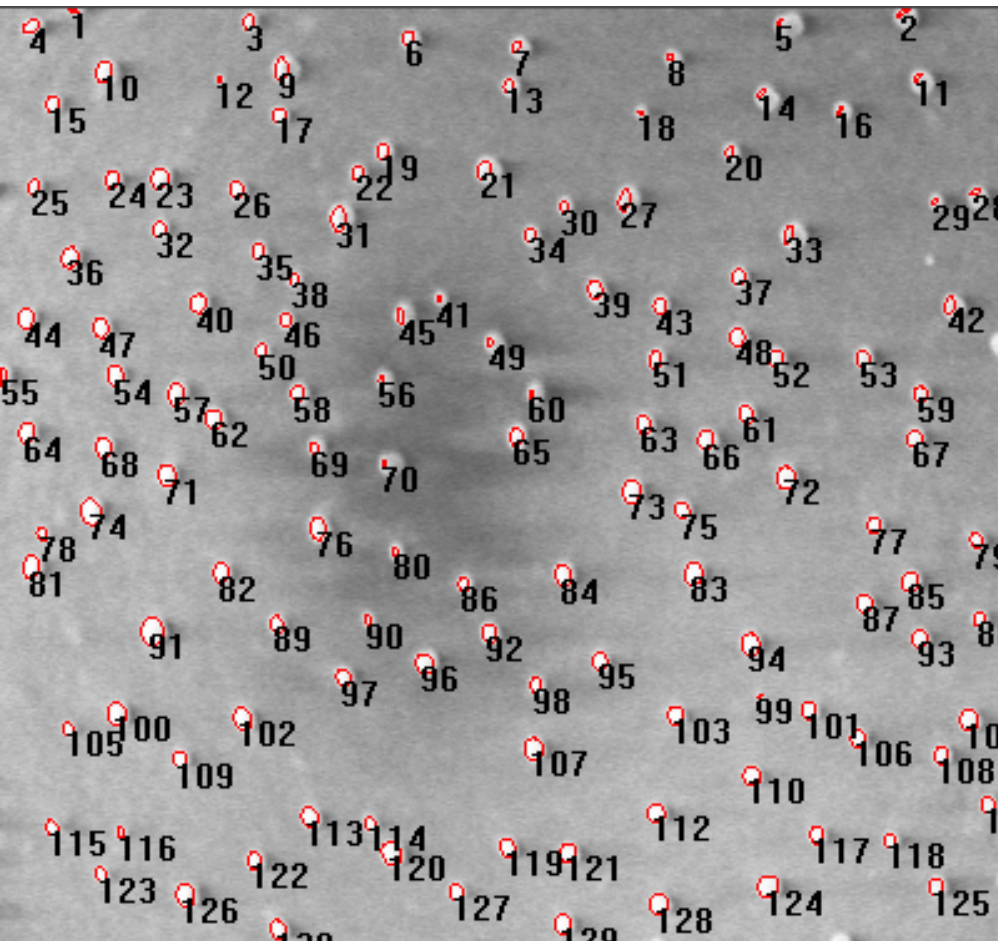
$$F_v = 6\pi\eta a v$$



Optical microscope images of different pairs of laser-trap connected microspheres *in vitro*. (100× object lens).



The average contact area between two microspheres were measured with the help of SEM image.

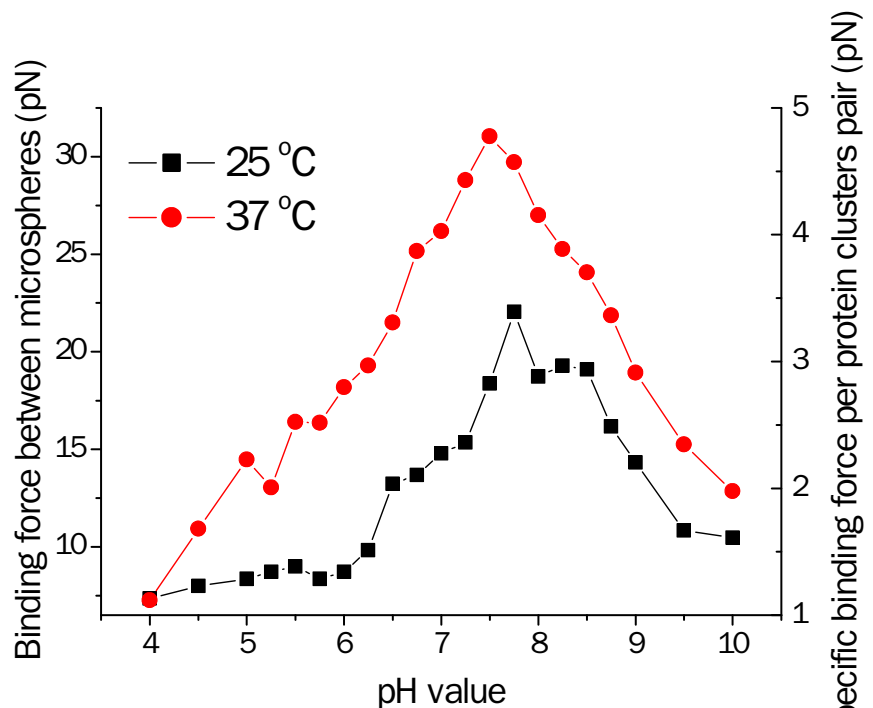


A $2\mu\text{m} \times 2\mu\text{m}$ SEM image of an anti-HBs-2 coated microsphere surface used for measuring the anti-HBs coating density.

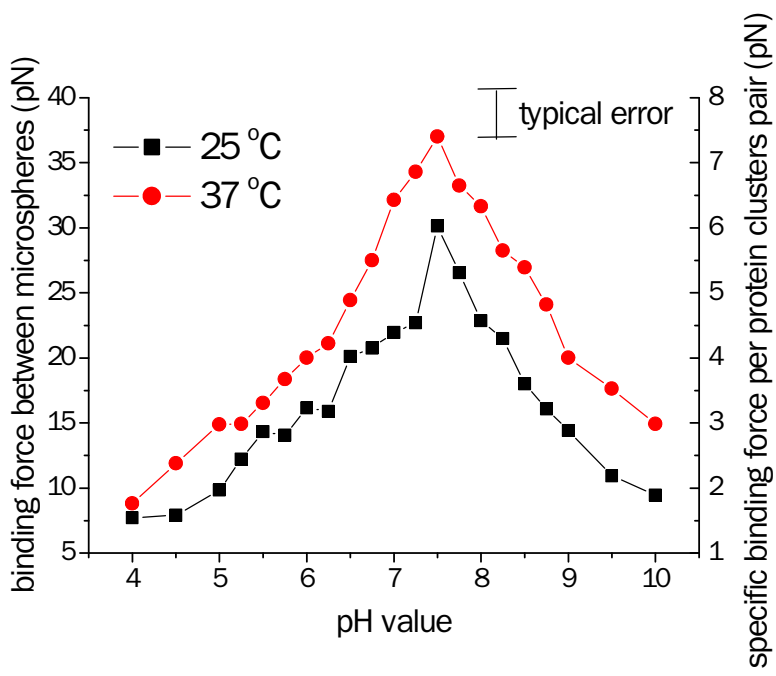
bonded protein pairs existed within the contact zone of each pair of microspheres:

Anti-HBs-1: 6.5 ± 0.3

Anti-HBs-2: 8.0 ± 0.2



Interaction between HBsAg
and anti-HBs-1.



Interaction between HBsAg
and anti-HBs-2.

Summary

- The HBsAg/anti-HBs interaction was found to be significantly influenced by the pH value of the surrounding medium as well as the experimental temperature, and at pH around 7.6, and temperature around 37 °C, strongest HBsAg/anti-HBs bonding is achieved.
- The experimental protocol used in present study to measure the interaction force of single antigen-antibody protein pairs was demonstrated, and this protocol can be employed to study other proteins, and can be adapted in industry applications

Case 4: Mechanical properties of leukemia cells studied by optical tweezers

What is leukemia?

- Cancer of the white blood cells
- Acute (blasts) or Chronic(close to mature cells)
- Affects ability to produce normal blood cells
- Bone marrow makes abnormally large number of immature white blood cells
- High mortality rates
 - Complication: Second malignancy
 - Leukostasis

Leukostasis

Leukostasis is a condition characterized by abnormal intravascular leukocyte aggregation and clumping. It is most often seen in leukemia patients.

Factors:

- Number of cells
- Deformability of cells
- Adhesion between cells and intravascular tissues



Chemotherapy may alter the mechanical properties of leukemia cells and cause Leukostasis --
Respiratory failure due to pulmonary leukostasis following chemotherapy of acute nonlymphocytic leukemia.

Myers et al. Cancer 1983

Drugs in treatment

- **PMA** is diester of phorbol and a potent tumor promoter often employed in biomedical research to activate the signal transduction enzyme protein kinase C (PKC).
- **All-trans retinoic acid (ATRA)** is the acid form of vitamin A. It is a drug commonly used to treat acne vulgaris and keratosis pilaris. It is also used to treat acute promyelocytic leukemia (APL).
- **Cytoxan,(CTX)**, An alkylating agent adds an alkyl group (C_nH_{2n+1}) to DNA. It is used to treat various types of cancer and some autoimmune disorders. It is a "prodrug"; it is converted in the liver to active forms that have chemotherapeutic activity.
- **Dexamethasone(DEX)** is used as a direct chemotherapeutic agent in certain hematological malignancies, especially in the treatment of multiple myeloma, in which dexamethasone is given alone or in combination with other chemotherapeutic drugs.
- Drug final concentration for exp. : PMA, 10ng/ml , ATRA, 1 μ M dexamethasone, 0.1 μ M, cyclophosphamide (CTX) : 20ug/ml

Deformability

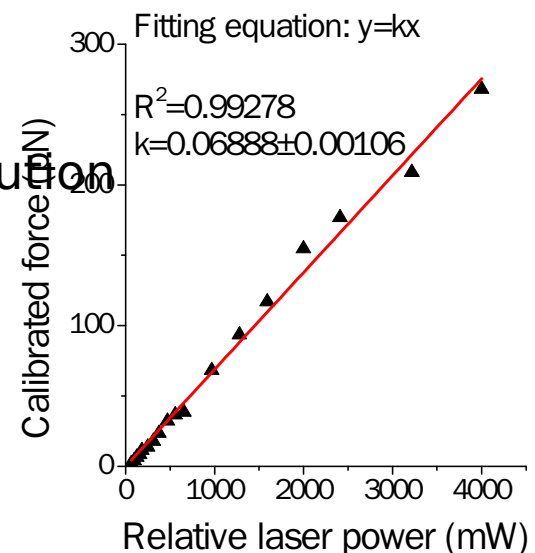
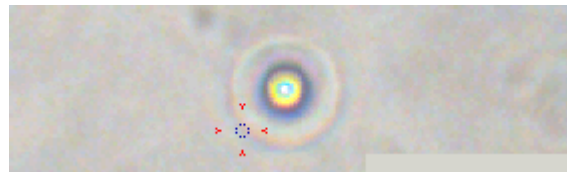
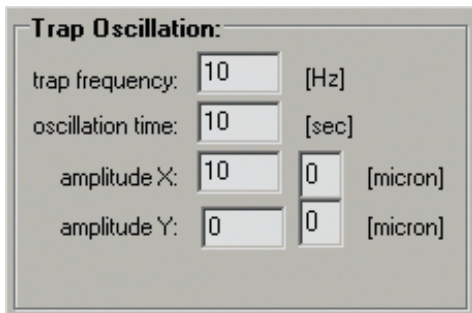
Optical tweezers

For laser power and force calibration, following the Citation
(Review of scientific instruments; 2007)

First using laser to trap microsphere and vibrate it periodically by rocking the laser beam. The critical frequency w and amplitude A_c are then used to calculate the maximum laser trapping force according to the equation

$$F_{\max}(x,t) = \sigma \eta a A_c f$$

Where η is the dynamic viscosity of the solution and α is the radius of the microsphere.

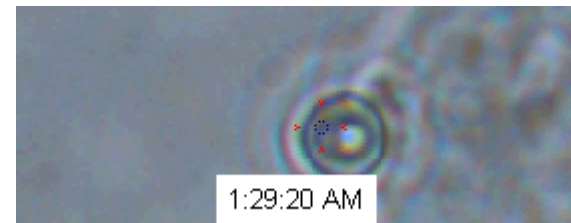


Indentation test performed by optical tweezers

Sneddon's elastic contact equation :

$$s = 2E_r a$$

where $s = \frac{dP}{dh}$ is the contact stiffness, a the contact radius a and E_r is elastic modulus. in this experiment, when the indentation depth h is large than the sphere radius r , the contact radius a should be a constant ($a=r$) and the s should also be a constant, and

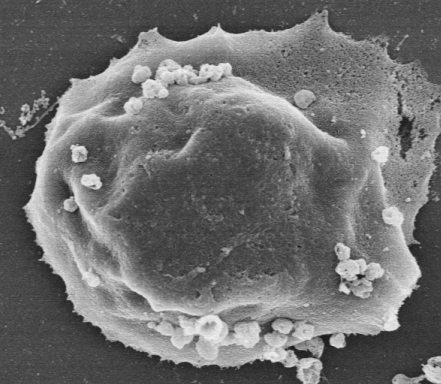


- The reduced modulus $\frac{E_r}{2wh_{max}}$ therefore can be calculated by:

Morphology of K562

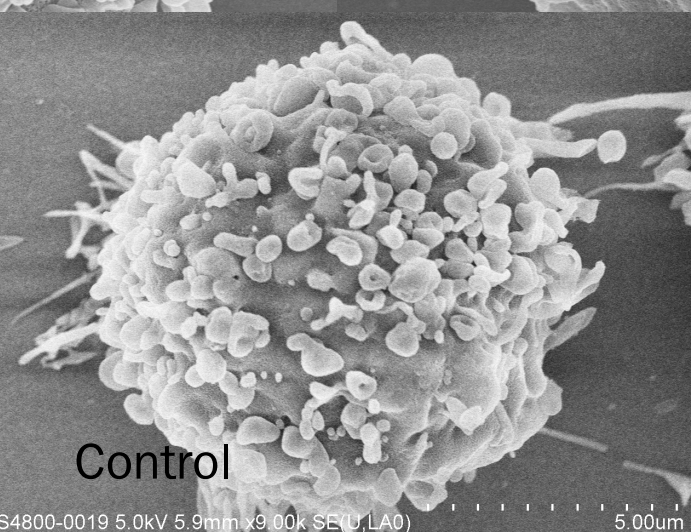
CTX
DEX

S4800-0049 5.0kV 5.8mm x8.00k SE(U)



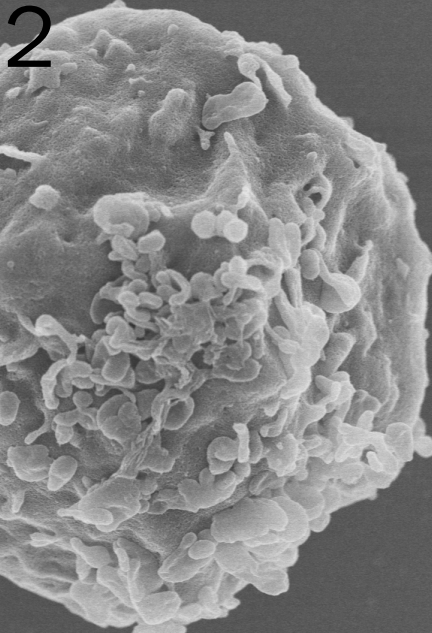
ATRA
MA

S4800-0041 5.0kV 5.7mm x4.00k SE(U)



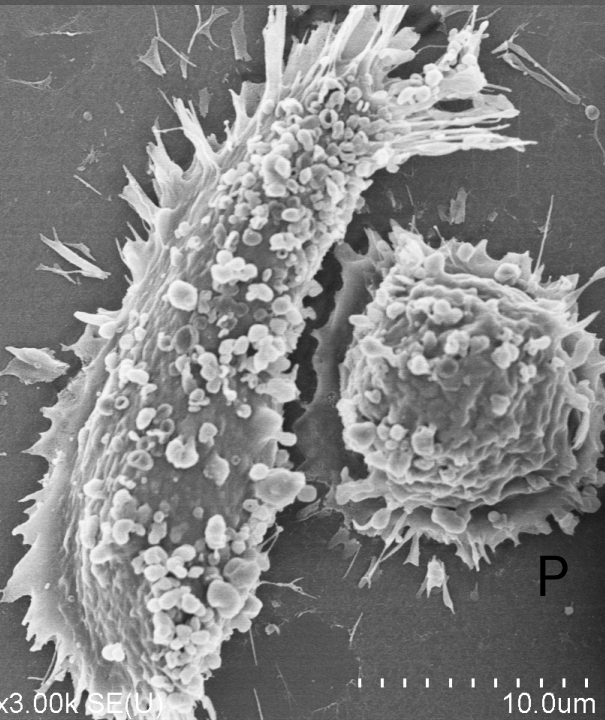
Control

S4800-0019 5.0kV 5.9mm x9.00k SE(U,LA0)



x8.00k SE(U)

5.00um



P

10.0um

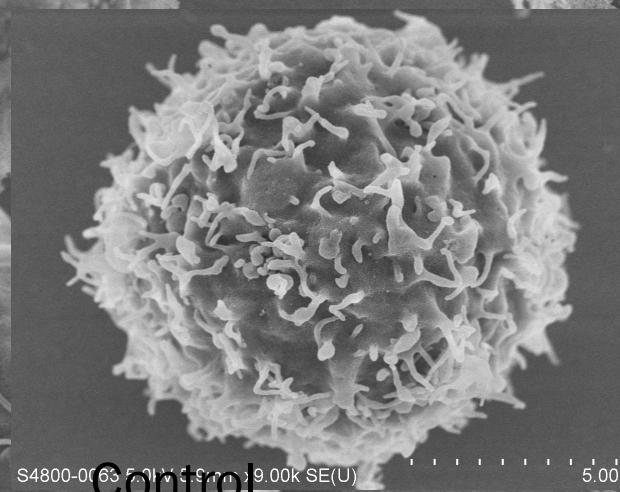
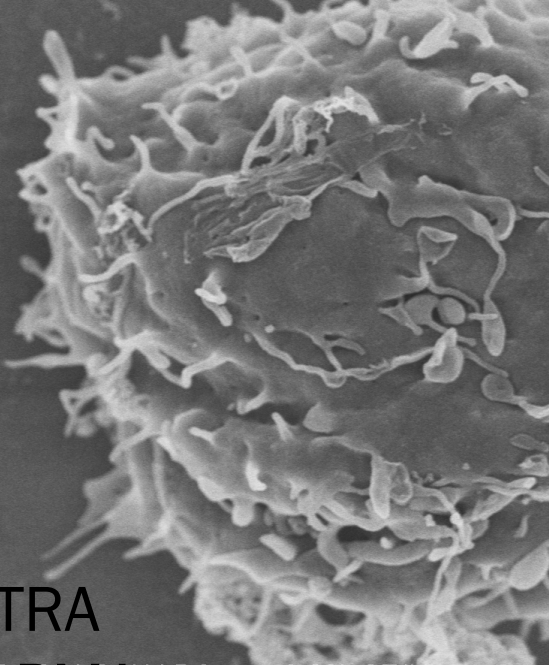
S4800-0032 5.0kV 5.8mm x3.00k SE(U)

10.0um

Morphology of HL60

CTX
DEX

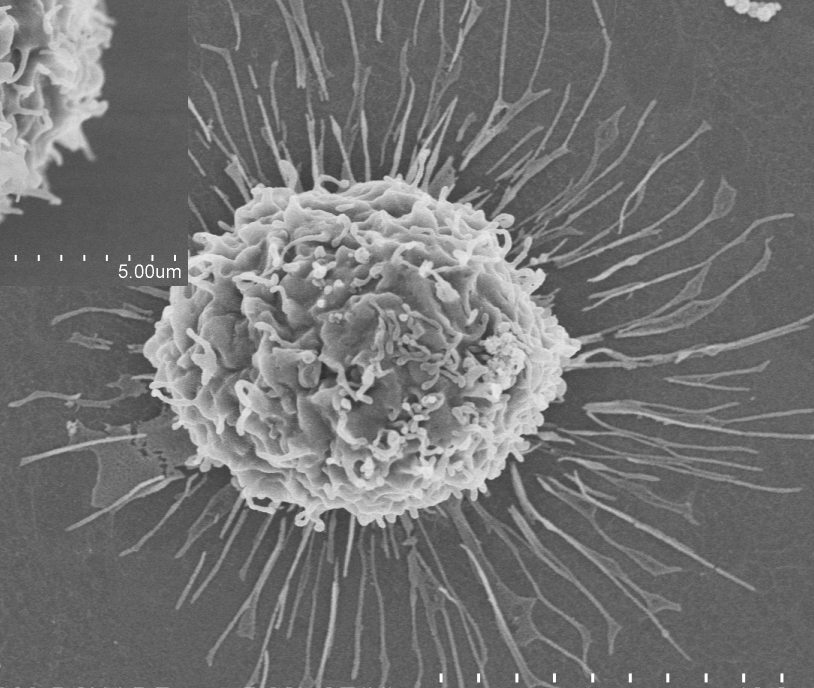
S4800-0079 5.0kV 5.6mm x10.0k SE(U)



Control

S4800-0063 5.0kV 5.9mm x10.0k SE(U)

5.00um



ATRA

S4800-0084 5.0kV 5.8mm x8.00k SE(U)

PMA

5.00um

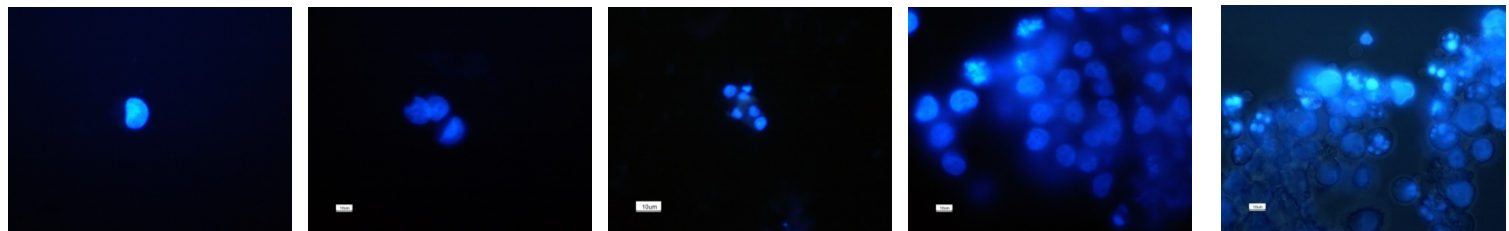
S4800-0069 5.0kV 5.7mm x5.00k SE(U)

10.0um

Reduced modulus in leukemic cells(n=12, mean \pm SD)

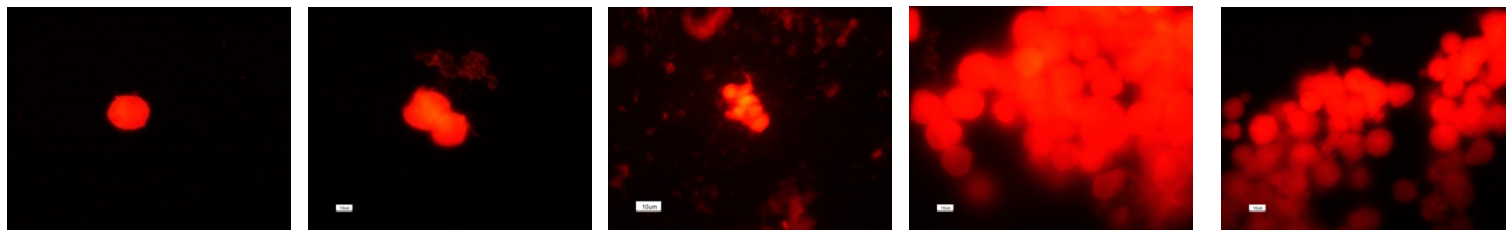
reduced Modulus (Pa)	Control	PMA	ATRA	DEX	CTX
K562	217 \pm 26	243 \pm 27	194 \pm 34	155 \pm 41	151 \pm 43
HL60	284 \pm 29	281 \pm 40	232 \pm 32	194 \pm 36	185 \pm 44

hoechst

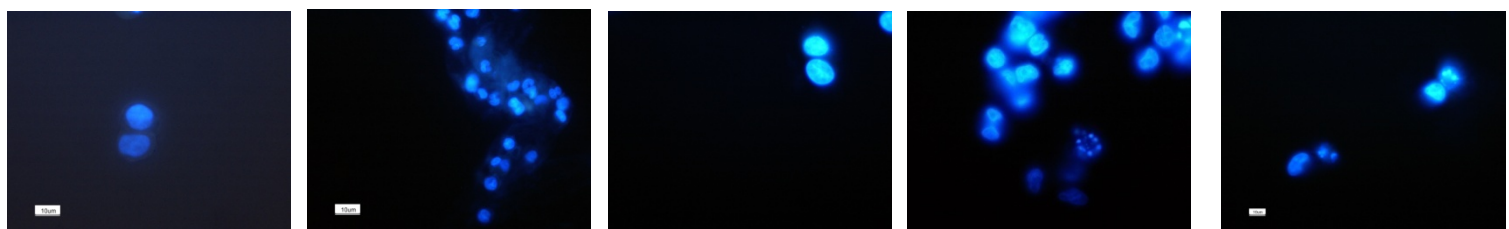


K562

phalloidin



hoechst



HL60

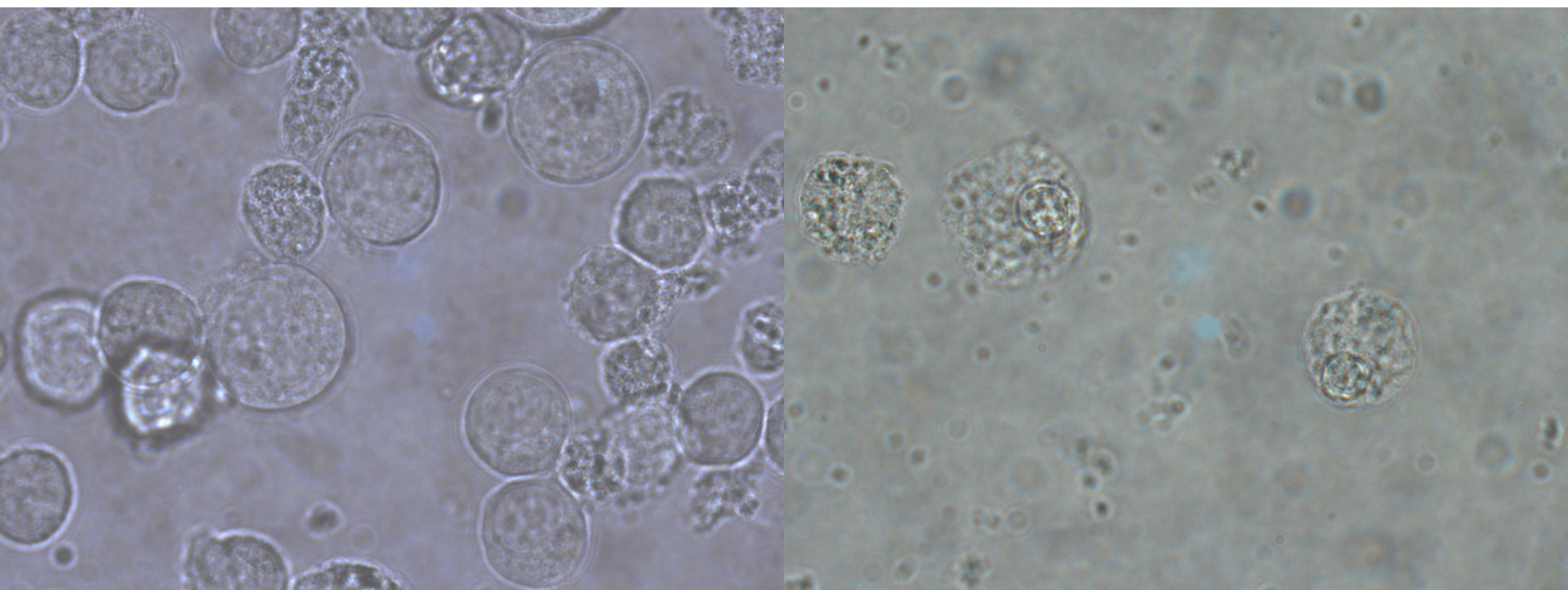
phalloidin

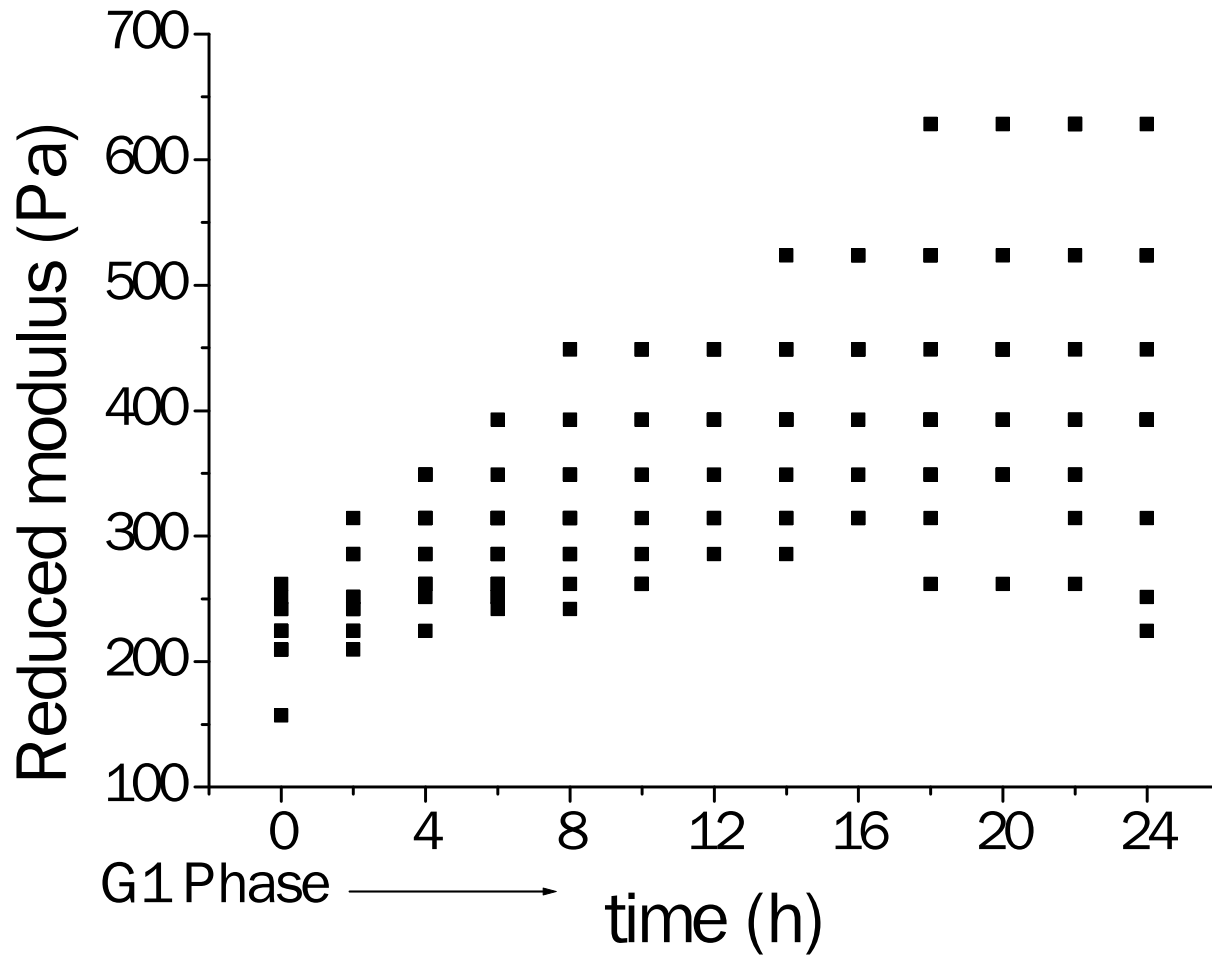


Mechanical properties vs. cell cycle

Synchronization is a process by which cells at different stages of the cell cycle are brought to the same phase

Nutritional deprivation: Elimination of serum from the culture medium for about 24 hours results in the accumulation of cells at G1 phase





Mechanical properties of K652 cells measured at different time point after Cell Synchronization

Case 5: Comparison of the Mechanical Properties of C57 and ICR Mice Femur Cortical Bone using Nanoindentation

Research background



C57 mice

VS.



ICR mice

A collaborative project with the Department of Orthopaedic Surgery
and Traumatology at HKU.

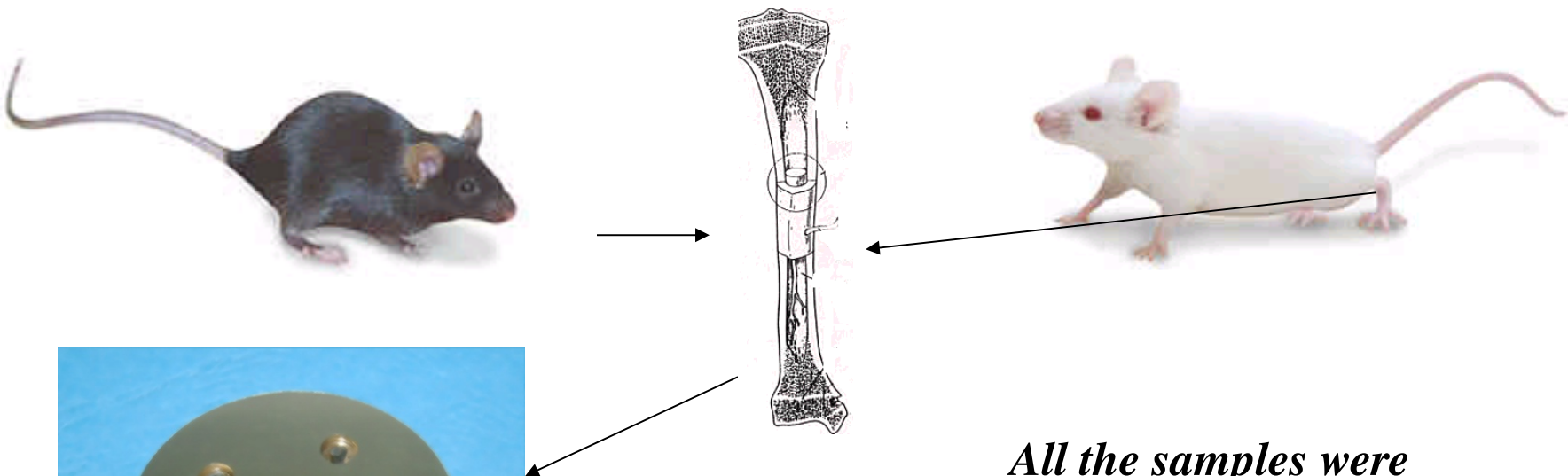
Experimental details

Samples used:

Cortical bone samples retrieved from different strains of mice femur

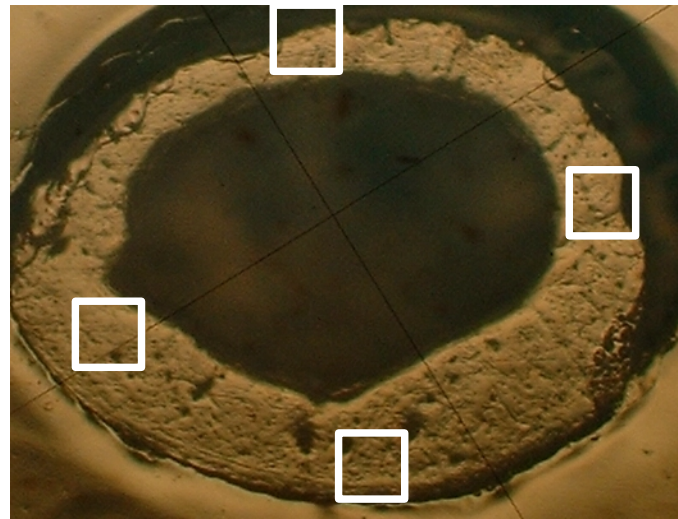
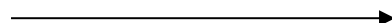
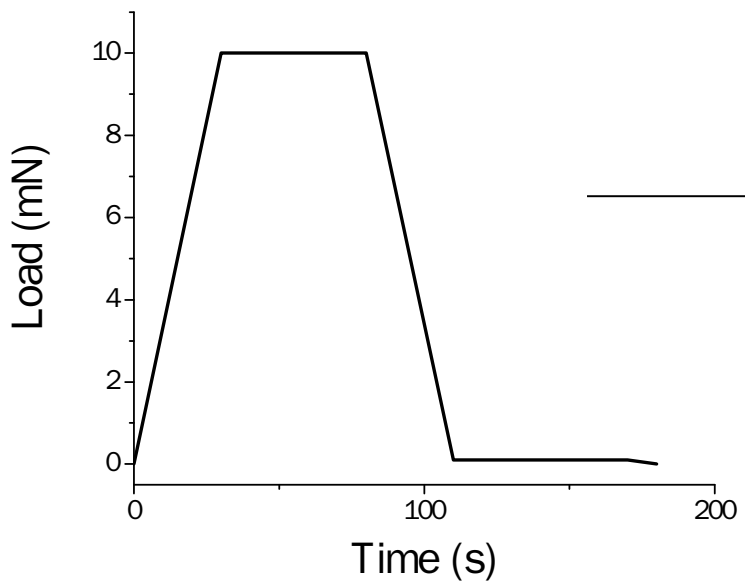
Analysis method:

The viscoelasticity correction method

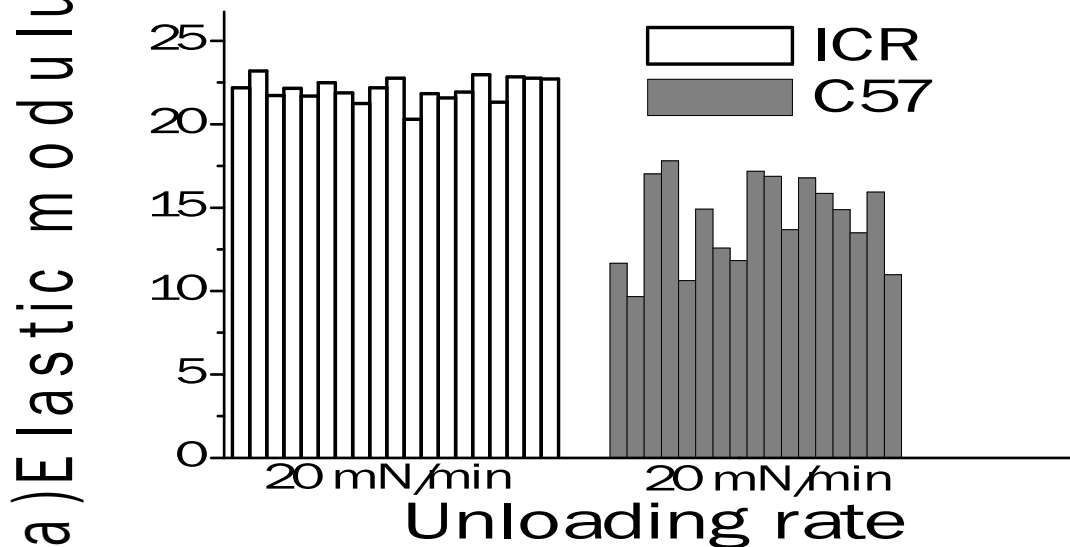


All the samples were embedded in same brass block and suffered similar mechanical polishing and dehydration.

Nanoindentation tests



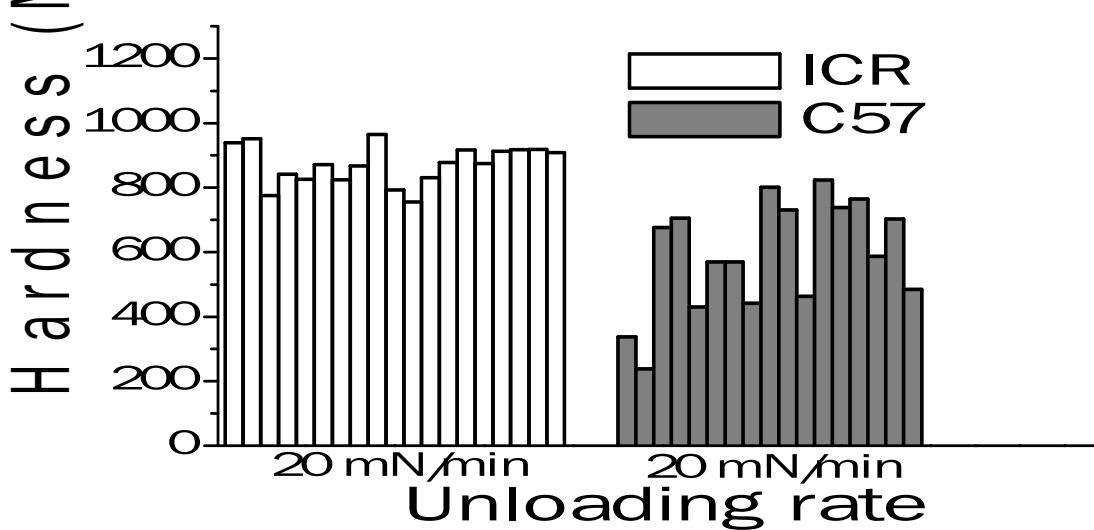
Results and discussions



Elastic modulus:

ICR: 22.09 ± 0.71 GPa

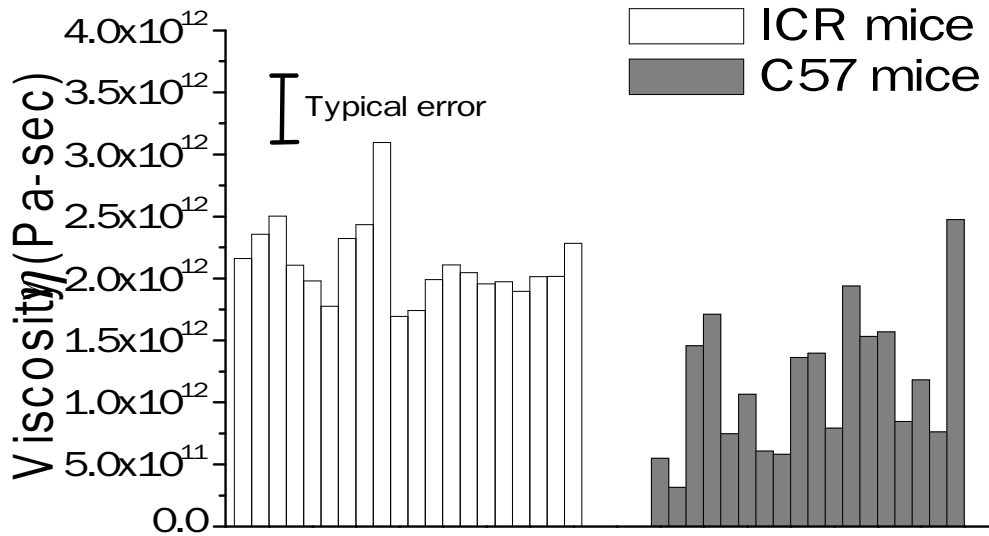
C57: 14.22 ± 2.61 GPa



Hardness:

ICR: 872.11 ± 60.10 GPa

C57: 592.13 ± 172.11 GPa



$$\eta = \frac{E_r P_h}{4(S_e h_h - \dot{P}_h)}$$

(Tang et al. 2006,
Philosophical Magazine)

Sample	Element	Element %	Ca: P
ICR 1	Ca	66.0	1.94
	P	34.0	
ICR 2	Ca	66.2	1.96
	P	33.8	
C57 1	Ca	52.4	1.10
	P	47.6	
C57 2	Ca	53.1	1.14
	P	46.8	

Chemical composition measured by EDAX

The higher ratio of calcium in the ICR bone sample correspond well to the better mechanical properties observed.

Conclusions

- . The tested ICR mice femur have higher elastic modulus, hardness and viscosity than C57 mice femur.**
- . The measured mechanical properties exhibit the expected correlation with the calcium content of the samples.**